KAON MASS BY CRITICAL ABSORPTION OF KAONIC ATOM X RAYS

by

GARY KONG LUM

A DISSERTATION

Presented to the Department of Physics
and the Graduate School of the University of Oregon
in partial fulfillment
of the requirements for the degree of
Doctor of Philosophy

DISCLAIMER

ACKNOWLEDGMENT

I would like to express my greatest humble appreciation to Dr. Clyde Wiegand who has taught me much in the realm of experimental physics. His teachings are beyond a doubt one of the best. Also I would like to thank Professor Emilio Segrè for allowing me to proof-read his entire first edition of Nuclei and Particles. Undoubtedly, proof-reading his text increased my knowledge in experimental and theoretical physics.

My appreciation also goes to the members of the LBL Nuclear Instrumentation Group for furnishing the Ge detectors, the Bevatron crew for providing the facilities for our experiment and Ben Galik for helping to run our experiment. Special thanks go to Professor Ryoichi Seki, Dr. Gary Godfrey and Professor C.S. Wu for lending us their computer cascade programs.

Finally I would like to thank my University of Oregon graduate advisor Professor David McDaniels, my parents and brothers and sister and my wife Anna for being patient in waiting so long for me to finish.

This work was supported by the U. S. Department of Energy under Contract W-7405-ENG-48.

TABLE OF CONTENTS

		page
I.	INTRODUCTION	1
II.	APPARATUS	6
	A. Beam	6
	B. Kaon Counters	9
	C. Targets	12
	D. X-ray Detectors	12
III.	PROCEDURES	16
IV.	SPECTRA ANALYSES	27
	A. Description of the Potassium X-ray Spectra	27
	B. Analysis of the Spectrum Without an Absorber	27
	C. Analysis of the Spectrum With an Absorber	35
V.	RESULTS OF CASCADE CALCULATION	38
	A. Description of a Mesonic Cascade Program	38
	B. Results	40
VI.	CONCLUSION	67
	REFERENCES	68

I. INTRODUCTION

The atoms of ordinary matter consist of a positively charged nucleus surrounded by a cloud of negatively charged electrons. Natural atoms range from hydrogen with one nuclear charge and one electron to uranium with 92 nuclear charges and 92 electrons. A more complex arrangement exists in exotic atoms. Exotic atoms are atoms in which an electron is temporarily replaced by another negatively charged particle. One type of exotic atom, a kaonic atom, is an atom where one of its electrons is replaced artificially by a negatively charged kaon.

A kaon when stopped in matter is believed to be captured in orbits of high radial quantum number n. It then cascades towards the nucleus by radiationless (Auger) transitions which are the most dominant mode for high n states. When the kaon reaches the low n states, radiation in the form of x rays dominate over the radiationless transitions. For sufficiently low ℓ states, the kaon interacts strongly with the nucleus. Nuclear force becomes stronger as the kaon cascades closer to the nucleus. At some low n state the cascade comes to a halt with the destruction of the kaonic atom. The kaon is absorbed by a nucleon and secondary reactions occur such as the emission of pions and hyperons.

The first kaonic x-ray spectra were observed by Wiegand and Mack[1] in 1967. Since then, measurements of kaonic x-ray lines of many elements throughout the periodic chart have been made by many groups, working at CERN,[2] Rutherford,[3] Berkeley,[4,5] and at Columbia.[6] For a general discussion on kaonic atoms one should see articles by Seki and Wiegand,[7] Burhop,[8] or Kim.[9]

The object of the presently described experiment is to measure the kaon mass by accurate determination of the energies of x rays emitted by kaonic atoms. The mass has been measured most accurately by Backenstoss et al.[10] (493.691 $\pm$ 0.040 MeV) and Cheng et al.[11] (493.657 $\pm$ 0.020 MeV). Their technique relied on the comparison of pulse heights of kaonic x-ray lines with the emission of calibrated radioactive sources. With this method there was no guarantee that the position of a pulse height could not be shifted due to background lines of low amplitude. We thought that it was appropriate to measure the x-ray energies by a different technique than had been employed in the above experiment, namely, determination of the x-ray energies by critical absorption.

The critical absorption technique is based upon the principle that the absorption coefficient μ/ρ is a steep function of photon energy when the energy matches closely the electron binding energy of the element. This technique is illustrated by an example shown in fig. 1 which shows the radiation absorption coefficient curve of the K edge of the element Er. The binding energy of the K-shell electron is located at the inflection point of this curve. When photons impinge on the Er foil with

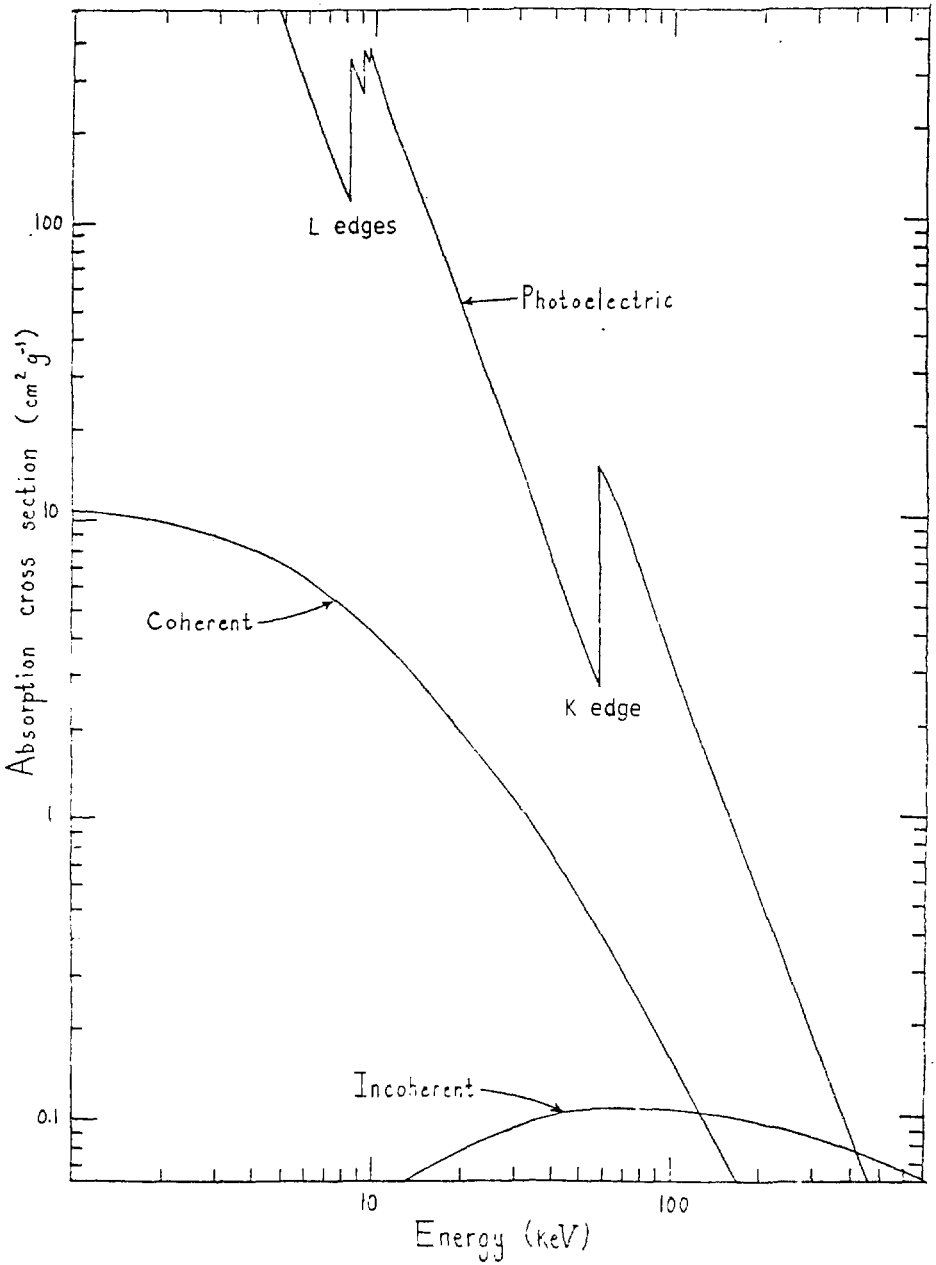

Fig. 1 Radiation absorption coefficient μ/ρ(cm^2/g) versus energy curve of the element Er. The binding energy of the K-shell electron is 57486 eV.

an energy located within the steep region of the curve, their energy E can be determined uniquely from the measured value of μ/ρ. Using tables of observed kaonic x-ray intensities and energies of x-ray absorption edges of the elements, we found that the intense kaonic transition 6h - 5g in potassium was within a few eV from the K electron binding energy of Er.

The energy levels of an exotic atom are related to the mesonic mass by the Dirac energy for point-like nuclei,

$$E_{n,j} = \mu c^2 \left[1 + \frac{(\alpha Z)^2}{\{ n-j-1/2 + [(j+1/2)^2 - (\alpha Z)^2]^{1/2} \}^2} \right]^{-1/2} ,$$

where $j = \ell \pm 1/2$, μ is the reduced mass, $\alpha = e^2/(\hbar c)$, and Z is the atomic number. For hadrons of zero spin, a substitution of $j = \ell$ reduces the expression to the Klein-Gordon energy. To the Klein-Gordon expression several corrections must be added. In order of importance these are the vacuum polarization, electron screening, nuclear finite size and strong interaction. The vacuum polarization correction depends on terms containing $\alpha(Z\alpha)$, $\alpha^2(Z\alpha)$, $\alpha(Z\alpha)^3, \ldots$. At the time this experiment was conceived, the calculations involving $\alpha^2(Z\alpha)^2$ were uncertain. For example, Min Y. Chen[12] calculated that this term for muonic Pb had the value of -35 eV, whereas, Wilets and Ringer[13] estimated a value < +3 eV. The calculated differences provided us with further impetus to perform the experiment. Our technique employed a low-Z element, whereas, previous precise determinations of the mass depended on elements of high-Z. The advantage of using a low-Z element reduced

<u>Case 2.</u> $T_r \geqslant T_c/2$

Partition the time interval T_c for detector A into the 3 intervals I, II and III, as shown in Fig. C.3. Similar to case 1, we have

$$C_I\ (T_r/T_c) = C_{III}\ (T_r/T_c) = \frac{3}{2}\ \frac{T_r}{T_c}\ .$$

For the interval II,

$$C_{II}\ (T_r/T_c) = 1\ .$$

Combining the contributions from I, II, and III we have

$$C\ (T_r/T_c) = \frac{T_c - T_r}{T_c}\ \frac{3\ T_r}{2\ T_c} + \frac{2\ T_r - T_c}{T_c} + \frac{T_c - T_r}{T_c}\ \frac{3\ T_r}{T_c}$$

$$= 2\ (T_r/T_c) - (T_r/T_c)^2 .$$

II. APPARATUS

A. Beam

Negative kaons were produced by bombarding a W target with 5.6 GeV/c protons at the Berkeley Bevatron. The Bevatron, a pulsed proton synchroton, generated an external beam intensity of about 5×10^{11} protons per pulse. The duration of each pulse was 1 second during each interval of 6 seconds.

The arrangement of the symmetrical mass spectrometer is shown in fig. 2. Bending magnet, M_1, dispersed horizontally negative kaons and pions, that were produced in the forward direction, and was adjusted so that 450 MeV/c particles would pass through the vertical momentum slit. Quadrupole Q_1 and the fringing field of the bending magnet were used to focus the beam. The separator deflected the focused beam to pass kaons through the horizontal mass slit. The different momenta that passed through the momentum slit were then recombined to a final focus in the second section.

The vertical electric field in separator S_1 operated at 500 kV per 10 cm. Vertical deflection through the separator is given by

$$d = \ell^2 qE \sqrt{[(m_0c^2)^2 + (pc)^2]} \; / \; [2(pc)^2] \quad , \qquad (1)$$

where p is the momentum, m_0 the rest mass, ℓ is the length of the separator (162 cm), q is the electron charge, and $\beta = v/c$. For example,

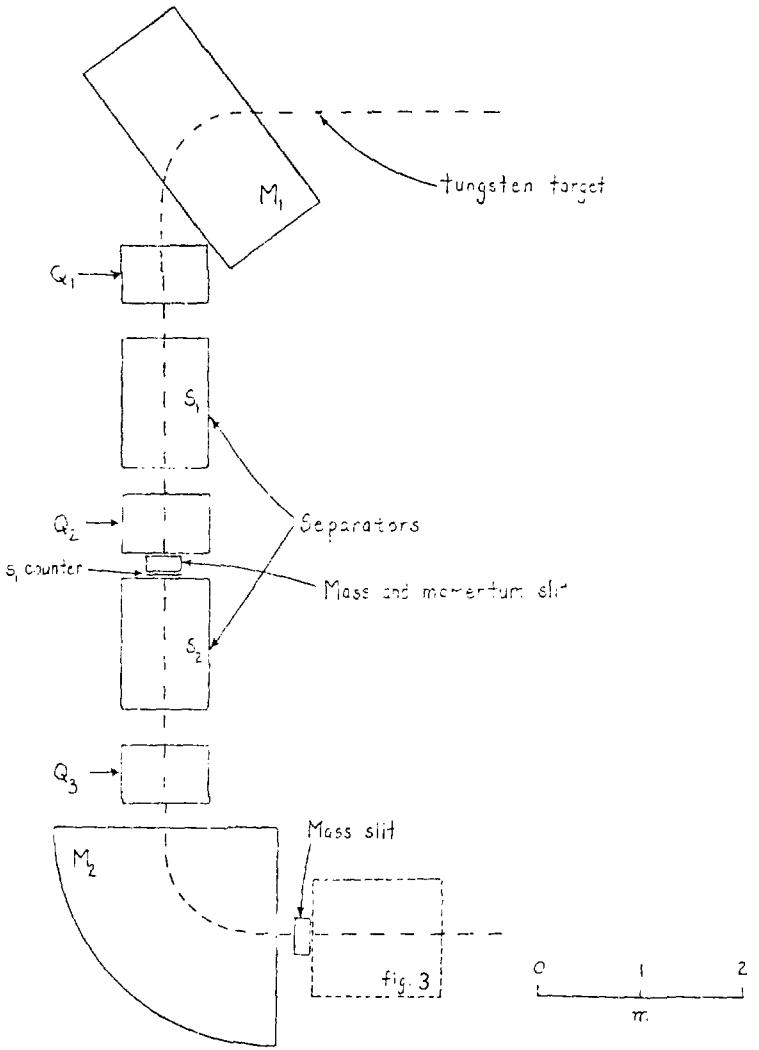

Fig. 2 Symmetrical mass spectrometer showing arrangement of quadrupole magnets Q_1, Q_2, Q_3, bending magnets M_1, M_2 and electrostatic separators S_1 and S_2.

at p = 450 MeV/c, pions were deflected less than kaons by about 0.5 cm. The separator was adjusted to pass kaons through the mass slit. The second section of the spectrometer operated in similar fashion to the first.

From eqn. 1 the deflection gets greater as the momentum p is decreased. However, as the momentum is lowered, more kaons are lost by decay. The length of time kaons spent in the beam is given by

$$t = D/(\beta c) \quad , \qquad (2)$$

where D (1001 cm) is the approximate length of the beam. The lifetime τ_0 of the kaon is 12.4 ns. Therefore, the number that survives along the beam is determined by

$$I = I_0 \exp(-t/(\tau_0 \gamma) \quad , \qquad (3)$$

where $\gamma = (1 - \beta^2)^{-1/2}$. A beam momentum of 450 MeV/c was choosen as a compromise between the effectiveness of the separation and the decay rate of the kaons in the beam. Beams for stopping kaons should be made as short as possible. For this reason, the fringing fields of the bending magnets were shaped to give vertical focusing in order to reduce the beam length. Even with our beam line, the fraction that survived was about 0.05. For a momentum of 450 MeV/c the range of kaons was 37 g/cm^2 of C. In order to bring the kaons to rest at the center of the target (2.8 g/cm^2), a total of 35.6 g/cm^2 was required. We noted that the range of 450 MeV/c pions amounted to 150 g/cm^2 of C. The beam of pions will not stop in the target except for a few that might be degraded by passing through part of the slit material.

At a proton beam intensity of 5×10^{11} per pulse, approximately 3×10^{7} pions entered the first mass separator. Due to chromatic aberrations and the scattering of pions from the beam components the spectrometer did not completely separate the pions and kaons. However, by using two mass separators, the pion intensity was reduced by a factor of 240, leaving 1.3×10^{5} pions in the beam.

B. Kaon Counters

A series of counters, forming a telescope was used to distinguish kaons from pions that were not separated by the mass spectrometer. The dimensions of the counters are listed in table 1. The arrangement of the counters and the target are shown in fig. 3.

At a momentum of 450 MeV/c, for pions $\beta = 0.955$ and for kaons $\beta = 0.674$. We used two methods to distinguish the velocities, namely, Čerenkov radiation and time of flight between S_1 and S_3 (fig. 2 and 3). The difference in time 7 ns over the flight distance of about 5 m was readily resolved by the coincidence circuits. The Čerenkov counter had a threshold of $\beta = 0.75$ and was connected in anticoincidence. Kaons stopped were identified by coincidences of S_1, $\bar{C}$, S_3, S_4, $\bar{S}_5$, where the bars designated that no counts occurred in C and S_5. S_5 was placed 33 cm away from the target in order that it would seldom trigger on charged particles that come from kaonic absorption in the nuclei of the target.

To verify the amount of degrader required and the momentum of the beam, a range curve was taken. We varied the amount of degrader to maximize the number of kaons that stopped in the target. The curve

Table 1. Counter dimensions

S_1	35 x 2.5 x 0.3 cm^3
C (Čerenkov)	15 x 15 x 6.7 cm^3
S_3	15.3 x 5.1 x 1.9 cm^3
S_4	7.6 cm diameter, 0.16 cm thick, covered on both sides with 0.0025 cm Al and 0.043 cm paper
S_5	13.5 x 8 x 1 cm^3

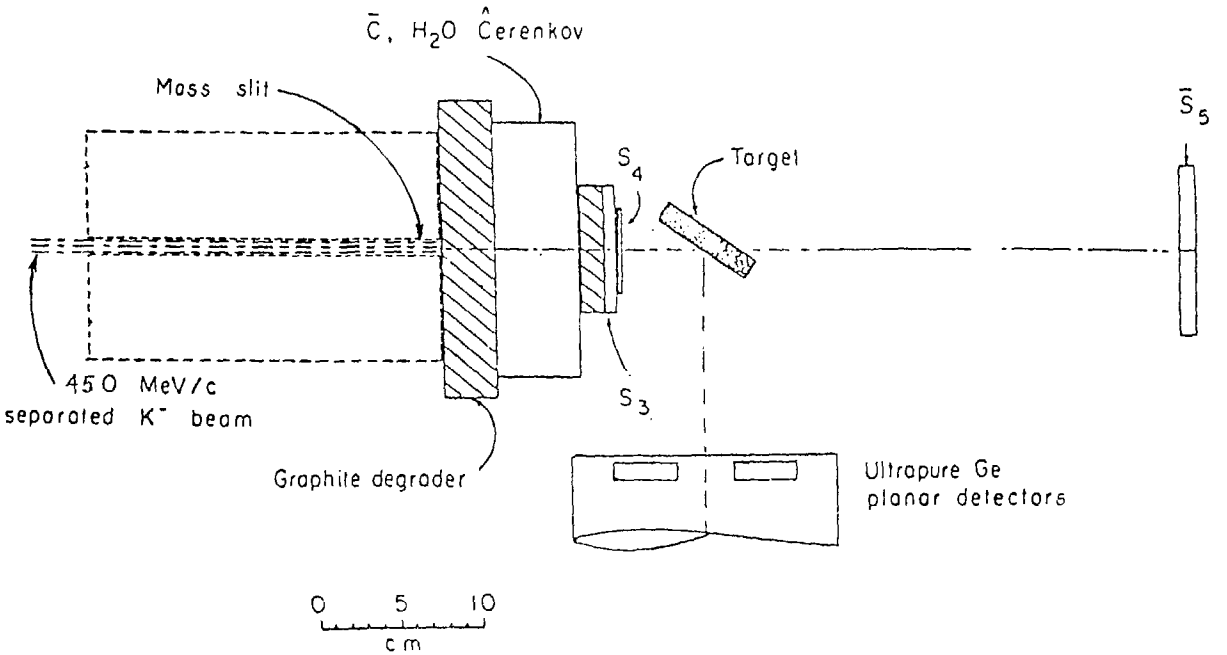

Fig. 3 Arrangement of the kaon counters, potassium target and Ge detectors. Counter S_1 is shown in fig. 2.

is shown in fig. 4 and shows the beam was 450 MeV/c. Less than 10^{-3} of the registered stopped kaons where due to pions.

C. Targets

The enriched potassium 41 target (0.9918 ^{41}K plus 0.0082 ^{39}K) was in the chemical form KF. The natural potassium (0.932 ^{39}K plus 0.068 ^{41}K) target was a metal. The targets were 6.34 cm in diameter and 1.75 g/cm^2 in thickness.

D. X-ray Detectors

The detectors consisted of crystals of ultrapure Ge. X rays entering in the Ge were mainly absorbed by the photoelectric process. The ejected electrons, whose ranges were short compared to the size of the crystal, lost energy by ionization in the form of electrons and holes. An external electric field was applied to the crystal to collect the charges. The number of charges collected was proportional to the energy of the x ray. A charge sensitive amplifier system was used to convert the number of charges to pulses whose height was proportional to the energy. The output pulses passed through a gate and into a multichannel analyzer. The gate was opened by a signal from the kaon counter described previously. After each run the content of the multichannel analyzer was stored on magnetic tape. The tape was processed later at the computer center. Fig. 5 shows two spectra.

If there were no noise in the system, the resolution full width at half maximum (FWHM) of a detector at a given energy would depend

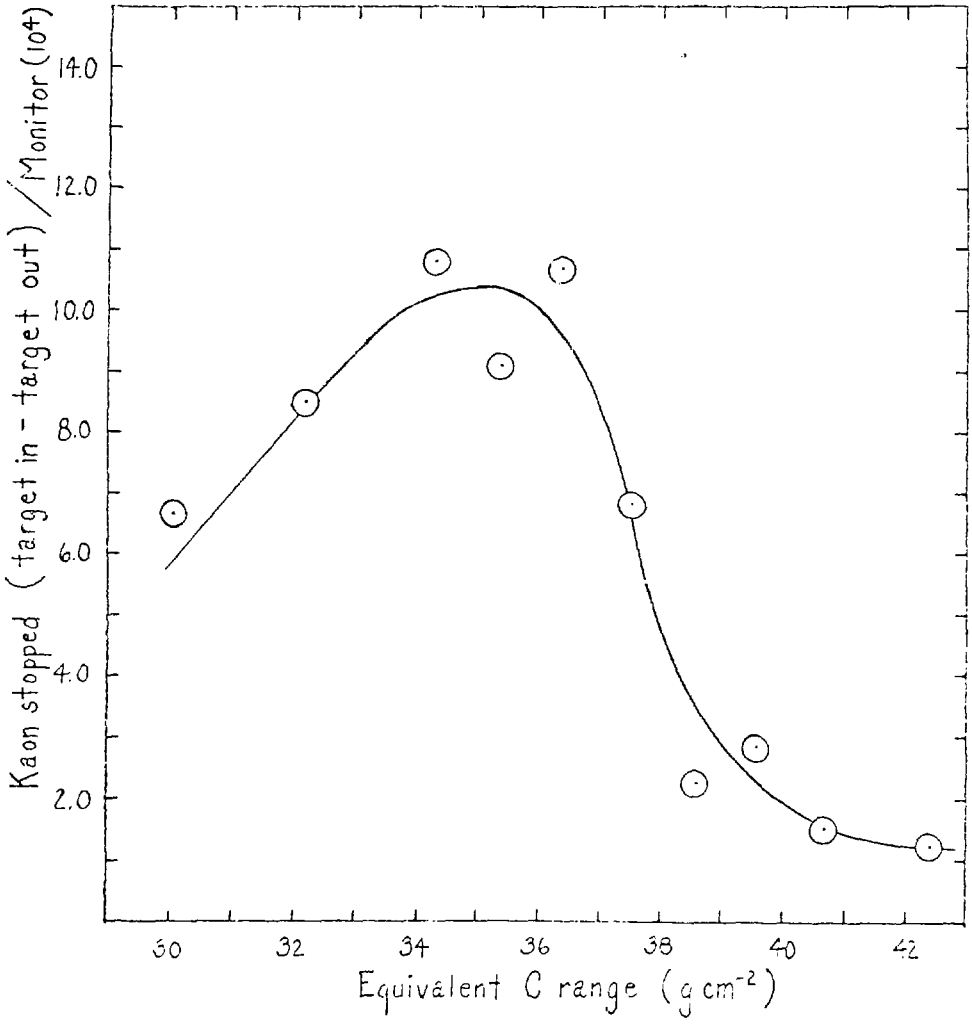

Fig. 4 Plot of stopped kaons versus thickness of equivalent graphite degrader.

Fig. 5 Kaonic natural potassium spectra with and without an absorber. Each spectrum corresponded to about 1.4 x 10^6 stopped kaons.

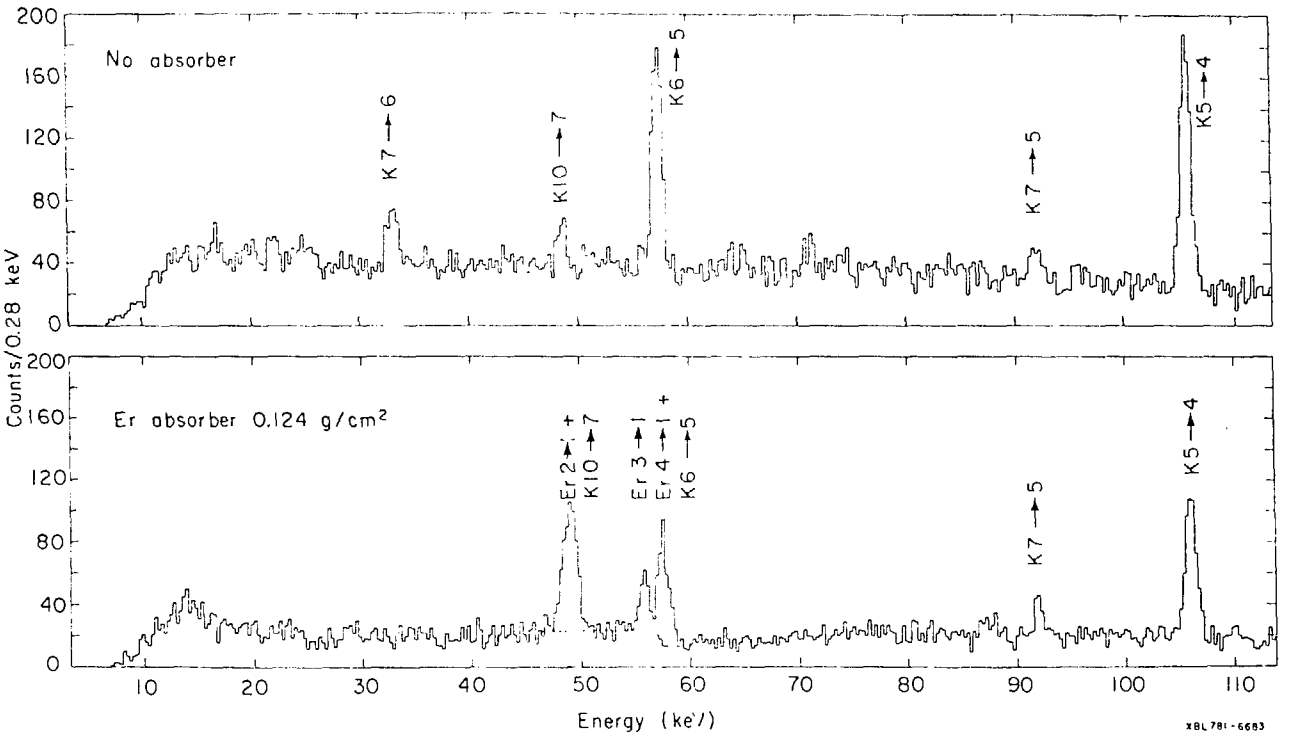

only on statistics:

$$\Delta E \text{ (FWHM)} = 2.36(E\varepsilon F)^{1/2} \quad , \tag{4}$$

where E is the energy deposited in the detector, ε is the average energy 2.94 eV to make an electron-hole pair in Ge, and F is the factor (Fano) due to the statistical nature of the ionization process. In the best detectors, F = 0.08.[21] The detectors used in this experiment had an F of approximately 0.1. However, in all electronic amplifiers there is a certain amount of random noise P, that adds in quadrature to the statistical fluctuation due to the Fano factor. The FWHM is given by

$$\Delta E \text{ (FWHM)} = [\ P^2 + (2.36)^2 E\varepsilon F\ ]^{1/2} \quad . \tag{5}$$

For example, at an energy of 81 keV, our detectors had a resolution of about 900 eV FWHM with the electronic noise contributing about 227 eV.

III. PROCEDURES

The geometrical setup is shown in fig. 6 and 7. Four ultrapure Ge detectors, 4 cm in diameter and approximately 1 cm thick, were located at the four corners of an imaginary 5.5 cm square whose center was directly below the target. Each of the Ge crystals was mounted on Al holders and was clamped in place around the top rim wi[illegible] BN ring 0.16 cm thick. BN served as an electrical insulator and a thermal conductor. The front surface of the Ge crystals had a coating of Pd a few angstroms in thickness for electrical contact. The detectors were located 0.32 cm below the Be window 0.157 cm thick. The distance between the center of the Be window and the center of the potassium target was 12.6 cm. At this distance the detectors were sufficiently out of the beam. The potassium target was inclined at 20 degrees with respect to the kaon beam line to maximize the number of kaons stopped and to minimize the effective thickness that x rays had to traverse in the potassium target.

The mounting for the target was made of lucite 0.635 cm thick. Care was taken to avoid introducing extraneous materials in the vicinity of the target which might generate x rays that would interfere with the kaonic potassium spectrum.

It was important that each absorber covered a detector completely in order that no radiation from the target could reach a detector

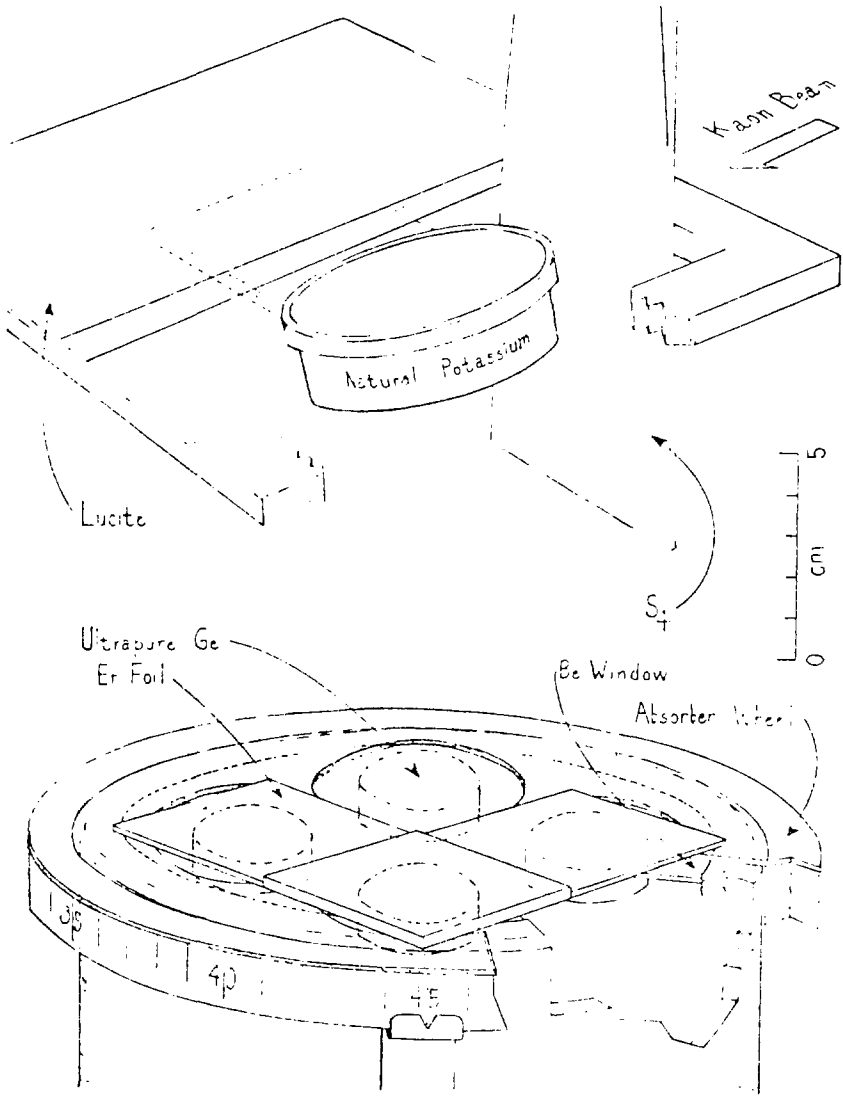

Fig. 6 Geometrical arrangement of the experiment.

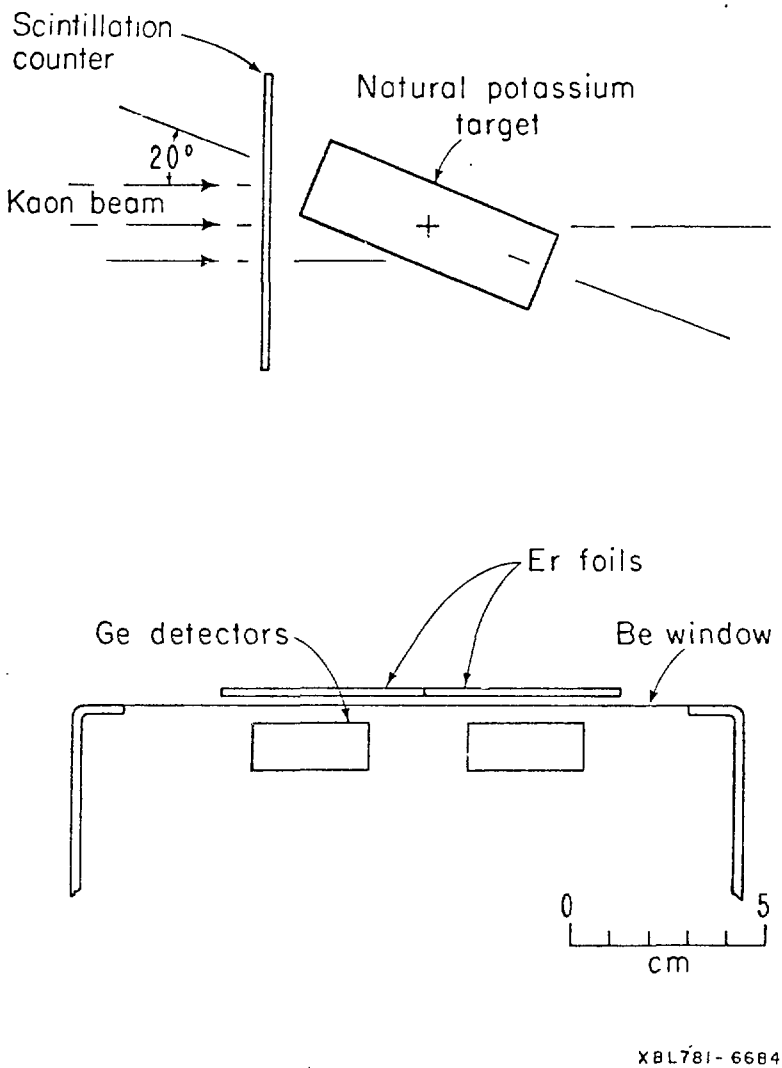

Fig. 7 Geometrical cross section of the experimental arrangement.

without passing through an absorber. In order to position the Er absorbers above the detectors, a wooden ring (16.5 cm inside diameter) covered by a 1 mm thick sheet of lucite was placed over the entire detector housing. The lucite sheet had four 7 cm diameter holes over which the absorbers were mounted. The circumference of the ring carried a scale so that the position of the wheel could be reproduced. Ring settings were determined in the following way. Pb foils, the same size as the Er foils (5 cm by 5 cm), were placed over three detectors. An ^{241}Am source was placed at the center of an empty target holder to simulate kaonic x rays. The Pb foils were sufficiently thick (1 mm) to shield the detectors from the ^{241}Am. As the ring was rotated, the Pb foils began to cover the fourth detector while another detector was being uncovered. The intensity of each detector was plotted versus ring settings and the results are shown in fig. 8. Ring settings were located at the centers of the regions where the intensities were minima.

At each proper setting of the ring, the ^{241}Am was moved to various positions over the entire target holder. This simulated the condition that kaons could stop uniformily in the potassium target. It was found that each Pb foil shielded the source completely from the detector over which the Pb foil was placed.

In order to establish how well our experiment could measure the mass absorption coefficient μ/ρ, we made the following measurements and compared the results with McMaster et al.[22] and Storm and Israel.[23] Sources less than 1 mm in diameter were centered 12 cm

Fig. 8 Plot of intensity of each detector versus absorber wheel setting. Pb foils were placed over three detectors while the fourth was exposed to a source. Ring settings were located at the centers of the regions where the intensities were minima.

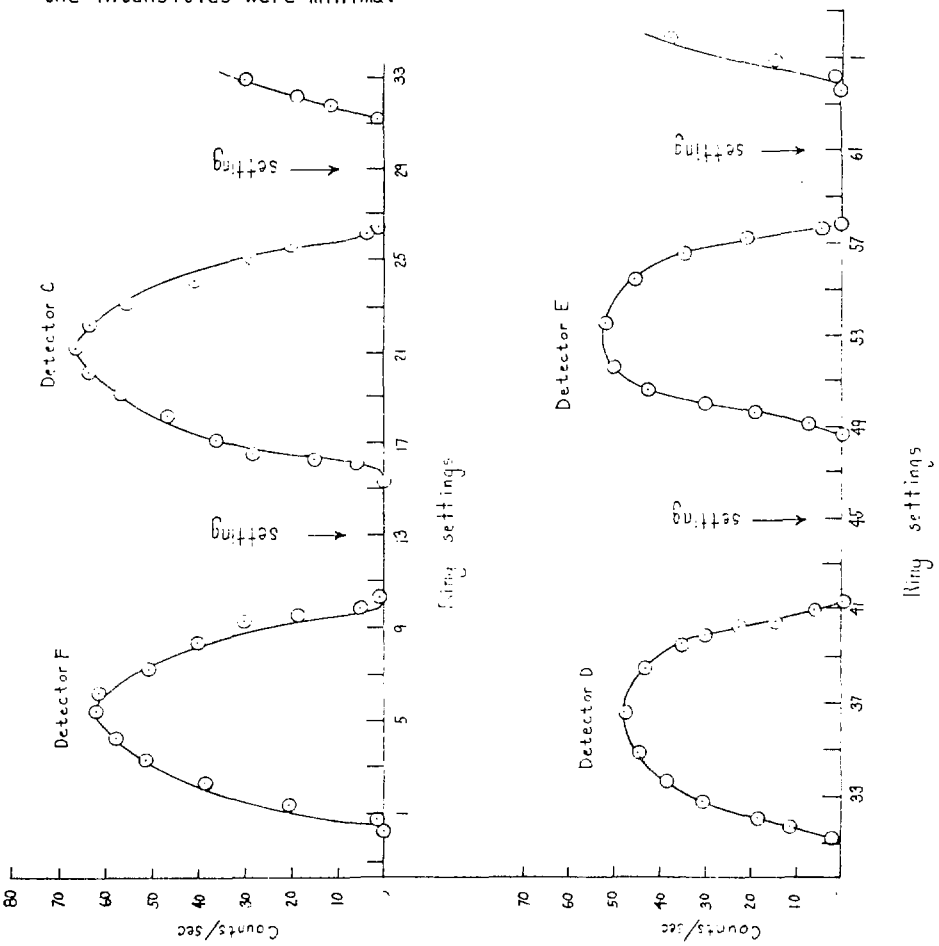

[illegible] single ultrapure Ge detector (3 cm in diameter by 1 cm thick). The mass absorption coefficient is given by

$$\mu/\rho(cm^2/g) = [\ln(I_0/I)] / t_{eff} \quad , \qquad (6)$$

where I_0 is the incident intensity, I is the attenuated intensity which passed through a foil and t_{eff} is the effective thickness of the foil. From the above arrangement it was evident that the apparent thickness of the foil would vary because radiation could penetrate at angles slightly different from normal incidence. An effective thickness must be used. As an approximation to t_{eff}, we assumed that radiation emitted by the source impinged on two concentric surfaces of equal areas of the detector. The angle of incidence at the boundary between the two areas was 5.05^0 and was used in t_{eff} which is given by

$$t_{eff} = t/\cos\theta_{av} \quad , \qquad (7)$$

where t is the actual foil thickness. For our experiment we had three Er foils (two of 0.123 g/cm^2 and one of 0.234 g/cm^2 thickness). The foils were sealed in Ar within two envelopes 5 cm by 5 cm made of 0.010 cm mylar. Spectra were recorded using a "blank" and the three absorbers. Table 2 lists our measured μ/ρ values. They agreed with McMaster et al.[22] and Storm and Israel[23] data which were the sum of the photoelectric plus incoherent mass absorption coefficients.

Having established that our measured Er mass absorption coefficient curve agreed with the McMaster et al.[22] or Storm and Israel[23]

Table 2. μ/ρ measurements of Er from sources (less than 1 mm in diameter) centered 12 cm in front of a single ultrapure Ge detector (3 cm in diameter by 1 cm thick).

Source	Energy (keV)	Apparent mass absorption coefficient (cm^2/g) with no correction to the obliquity of x rays; $t_{eff} = t$	$t_{eff} = \frac{t}{\cos(5.05^0)}$	McMaster et al.[22]	Storm and Israel[23]
^{133}Ba	53	3.608 ± 0.050	3.594 ± 0.049	3.49	3.50
	81	5.937 ± 0.017	5.914 ± 0.017	6.065	5.80
^{241}Am	59.5	13.73 ± 0.03	13.68 ± 0.03	13.711	13.56
^{232}Th K_{α_2}	89.96	4.505 ± 0.060	4.488 ± 0.070	4.58	4.58
K_{α_1}	93.4	4.23 ± 0.05	4.21 ± 0.05	4.15	4.20
$K_{\beta_1'}$	105	3.04 ± 0.09	3.02 ± 0.09	3.04	3.05
^{122}Co	122	2.056 ± 0.025	2.048 ± 0.025	2.05	2.10

table, we proceeded to determine the effective thickness for the Er foils for the four-detector arrangement where the sources were not positioned over the center of the detectors. Sources 1 mm in diameter were placed at the center of the empty target holder. The Pb foils on the ring were replaced by the three Er foils (two of 0.123 g/cm^2 and one of 0.246 g/cm^2 thickness). After the ring was set at each proper setting, a set of four spectra were recorded for each detector. I_0 and I were obtained from the four spectra. Table 3 lists the effective incident angles used in t_{eff} in order to calculate μ/ρ which agreed with the measured values in table 2. A weighted average of the effective incident angles of each detector was then used in the measurement of μ/ρ for the kaonic 6g - 5h transition.

Because the actual distribution of stopped kaons in the target was not known, we rotated the absorber wheel about every 12 hours of running so that geometrical effects would average out. The absorber wheel was rotated to the proper settings for an accumulation of about 0.7×10^6 stopped kaons. When the natural potassium target was placed in the target holder, Er foils (two of 0.123 g/cm^2 and one of 0.234 g/cm^2 thickness) were mounted over three of the four holes of the absorber wheel. For the potassium-41 target, Er foils (0.123 g/cm^2) were mounted over two holes, while the other holes remained uncovered. For the natural potassium each detector collected about 96 hours of beam time and for potassium-41 48 hours was collected. At the end of each period, readouts of several electronic pulse scalers were recorded both for bookkeeping and diagnostic pur-

Table 3. Effective incident angles of radiation on the four detector arrangement where the sources were not positioned over the center of the detectors. The values of $\mu/\rho_{meas.}$ were taken from table 2.

Source	$\mu/\rho(cm^2/g)$ meas.	Θ_{eff} of detector:			
		C	D	E	F
^{241}Am	13.68 ± 0.03	14 ± 1°	13 ± 1°	17 ± 1°	13 ± 1°
^{133}Ba	5.914 ± 0.017	12 ± 1°	18 ± 1°	18 ± 1°	17 ± 1°
	averaged Θ_{eff} :	13.0 ± 0.7°	15.5 ± 0.7°	17.5 ± 0.7°	15.0 ± 0.7°

poses. Table 4 is an example of the numbers recorded. Data tapes were processed at the LBL computer center where the results of the numbers of events in each pulse-height channel were printed and plotted out. Fig. 5 are examples of spectra of the detector uncovered and covered by an Er absorber. In this section we have discussed the procedures to measure the absorption coefficients which were used to determine the energies of the x rays from which the kaon mass was calculated.

Table 4. Numbers recorded after each 12 hours of beam time. S_3 counted mostly pions. $K_{stopped}$(true) were identified by coincidences of S_1, $\bar{C}$, S_3, S_4, $\bar{S}_5$, where the bars designated that no counts occurred in C and S_5.

Absorber wheel setting with $^{39}_{19}K$	Bevatron bursts	S_3 (10^6)	$K_{stopped}$(true) (10^6)	Er absorbers (g/cm^2) covering detectors: C	D	E	F
13.3	6527	855.063	0.700	0.237	0.123	0.1238	0
29.0	4350	828.235	0.720	0	0.237	0.123	0.1238
45.3	4224	888.916	0.734	0.1238	0	0.237	0.123
61.3	4347	684.667	0.555	0.123	0.1238	0	0.237
Absorber wheel setting with $^{41}_{19}K$							
29.0	6250	1119.616	1.001	0	0	0.123	0.1238
61.3	6523	1178.533	0.976	0.123	0.1238	0	0

IV. SPECTRA ANALYSES

A. Description of the Potassium X-ray Spectra

In the spectra shown in fig. 5 our task was to analyze the K^- $n = 6 \rightarrow 5$ to determine its absorption coefficient μ/ρ. The Er fluorescence lines that were present when an absorber was over a detector came from electrons that made either $n = 2 \rightarrow 1$, $n = 3 \rightarrow 1$, or $n = 4 \rightarrow 1$ transitions. Atomic spectroscopists generally refer to these electronic x-ray lines as the K_{α_2}, K_{α_1}, $K_{\beta_1'}$, $K_{\beta_2'}$ of energies 48.2, 49.1, 55.6 and 57.2 keV, respectively. The relative intensities of the K_{α_1}, K_{α_2}, $K_{\beta_1'}$ and $K_{\beta_2'}$ lines are 100: 53: 32: 7.[24] From these relative intensities $K_{\beta_1'} / [K_{\alpha_1} + K_{\alpha_2}] = 0.209$ and $K_{\beta_2'} / [K_{\alpha_1} + K_{\alpha_2}] = 0.046$. Our measured intensities for the above ratios were $K_{\beta_1'} / [K_{\alpha_1} + K_{\alpha_2}] = 0.199 \pm 0.003$ and $K_{\beta_2'} / [K_{\alpha_1} + K_{\alpha_2}] = 0.047 \pm 0.002$ We compared these ratios because they would be used in the analysis later. Three other lines present in the 57.5 keV region were the K^- $n = 10 \rightarrow 7$, K^- $n = 8 \rightarrow 6$ and the Σ^- $n = 4 \rightarrow 3$ of energies 48.8, 57.0 and 53.3 keV, respectively.

B. Analysis of the Spectrum Without an Absorber

The spectrum without an absorber was analyzed in the following way. An energy scale was established based on the observed energies

of the prominent lines.[25] From the energy scale we could locate the centroids of the Er fluorescence lines, the K^- n = 10 → 7, K^- n = 8 → 6 and the Σ^- n = 4 → 3. Although the spectrum without an absorber should not have shown any Er fluorescence x rays when no absorbers were over the detectors, the electronic n = 4 → 1 which could not be resolved from the K^- n = 6 → 5 still appeared with counts amounting to about 1% of the K^- n = 6 → 5. The reason was that the detectors were close to each other and fluorescences from the absorbers themselves were able to leak into an adjacent detector that was or was not covered by an absorber.

The background was established by using a straight sloping background for the 57.5 keV region. The background was determined by taking a combined background averaged over a 1 keV range from the low energy side of the K^- n = 10 → 7 and from the high energy side of the K^- n = 6 → 5.

To find the amount of fluorescence x rays under the K^- n = 6 → 5 due to the leakage, it was necessary to first determine the number of electronic K_αs'. To determine the number of counts under a spectral line at least plus or minus three standard deviations ($\pm 3\sigma$) from its centroid was used. The K_{α_2}, K^- n = 10 → 7, and K_{α_1} peaks were combined by including counts at least -3σ below the K_{α_2} and $+3\sigma$ above the K_{α_1}. The $K_{\beta_1'}$, $K_{\beta_2'}$, K^- n = 8 → 6, and K^- n = 6 → 5 were combined by including counts $\pm 4\sigma$ from the K^- n = 6 → 5. Minus three standard deviations could not be taken from the $K_{\beta_1'}$ because the range would

include the Σ^- n = 4 → 3 peak.

In order to determine the number of K^- n = 10 → 7 present, the intensity ratio

$$\frac{K^- \; n = 10 \rightarrow 7}{K^- \; n = 6 \rightarrow 5 \; + \; K^- \; n = 8 \rightarrow 6} = 0.0904 \pm 0.0144 \quad , \quad (8)$$

determined from Godfrey's work[25] was used. Since $K_{\beta_1'}$ and $K_{\beta_2'}$ together contributed less than 5% of the counts in the above consolidated peak, the $K_{\beta_1'}$ and $K_{\beta_2'}$ contributions were neglected in determining the number of K^- n = 10 → 7 from the above ratio.

$$N_{K^- \; n = 10 \rightarrow 7} = (0.0904 \pm 0.0144) \times (N_{K_{\beta_1'} + K_{\beta_2'} + K^- \; n = 8 \rightarrow 6 \; + \; K^- \; n = 6 \rightarrow 5}) \quad , \quad (9)$$

The number of K^- n = 10 → 7 was then subtracted from the combined K_αs' + K^- n = 10 → 7 in order to determine the amount of K_αs' present caused by the Er fluorescences entering an adjacent detector,

$$N_{K_{\alpha_1} + K_{\alpha_2}} = N_{K_{\alpha_1} + K_{\alpha_2} + K^- \; n = 10 \rightarrow 7} - N_{K^- \; n = 10 \rightarrow 7} \quad . \quad (10)$$

Since three of the detectors (C, D and F) resolved the $K_{\beta_1'}$ from the K^- n = 6 → 5 + K^- n = 8 → 6, the $K_{\beta_1'}$ peak was hand counted carefully. For the other detector (E), our measured ratio $K_{\beta_1'}$ / [K_{α_1} + K_{α_2}] = 0.199 ± 0.003 multiplied by the K_{α_1} + K_{α_2} intensity was used to obtain $K_{\beta_1'}$. For the unresolvable $K_{\beta_2'}$, $K_{\beta_2'}$ / [K_{α_1} + K_{α_2}] =

0.047 ± 0.002 of the $K_{\alpha_1} + K_{\alpha_2}$ intensity was used. The number of $K_{\beta_1'}$ and $K_{\beta_2'}$ was then subtracted from the combined $K_{\beta_1'} + K_{\beta_2'} + K^- n = 8 \rightarrow 6 + K^- n = 6 \rightarrow 5$ to determine the $K^- n = 8 \rightarrow 6 + K^- n = 6 \rightarrow 5$.

The number of $K^- n = 6 \rightarrow 5$ was found by using the ratio

$$K^- n = 8 \rightarrow 6 \;/\; [\, K^- n = 6 \rightarrow 5 + K^- n = 8 \rightarrow 6 \,] = 0.091 \pm 0.020 \,, \tag{11}$$

which was determined in the following way. Table 5 contains S, Cl, Ar, potassium and Ca intensities from Godfrey's measurements.[25] We see that a $\Delta n = 2$ intensity is about 12% of the $\Delta n = 1$. By assuming that the kaonic cascade contributed no anomalous irregularities to the $n = 8 \rightarrow 6$, we assumed that weighed averages could be taken among these elements. The ratio $K^- n = 8 \rightarrow 6 \,/\, K^- n = 6 \rightarrow 5$ was assumed to be the same as a weighed average of the $K^- n = 9 \rightarrow 7 \,/\, K^- n = 8 \rightarrow 7$ with the $K^- n = 6 \rightarrow 4 \,/\, K^- n = 5 \rightarrow 4$, and $K^- n = 8 \rightarrow 6$ was assumed to be the same as a weighed average of the $K^- n = 7 \rightarrow 5$ with the $K^- n = 9 \rightarrow 7$. From the $K^- n = 8 \rightarrow 6 \,/\, K^- n = 6 \rightarrow 5$ ratio the $K^- n = 6 \rightarrow 5$ absolute intensity was calculated and then combined with the $K^- n = 8 \rightarrow 6$ to determine $K^- n = 8 \rightarrow 6 \,/\, [\, K^- n = 8 \rightarrow 6 + K^- n = 6 \rightarrow 5 \,]$ as given above.

Table 6 lists the yields of $K^- n = 10 \rightarrow 7$, $K_{\alpha_1} + K_{\alpha_2}$, $K_{\beta_1'} + K_{\beta_2'}$, $K^- n = 8 \rightarrow 6$, and $K^- n = 6 \rightarrow 5$ measured for each detector without an absorber. These yields should be normalized by the appropriate numbers

Table 5. Kaonic x-ray intensities (x rays per stopped kaons) from certain transitions measured by G.L. Godfrey.[25]

Transition	$n = 9 \rightarrow 7$	$n = 7 \rightarrow 5$	$n = 6 \rightarrow 4$	$n = 8 \rightarrow 7$	$n = 5 \rightarrow 4$
Element					
S		0.040 ± 0.002	0.039 ± 0.002		0.361 ± 0.004
Cl (CCl_4)	0.035 ± 0.015	0.037 ± 0.002	0.036 ± 0.002	0.514 ± 0.108	0.355 ± 0.004
Ar		0.044 ± 0.006	0.050 ± 0.008		0.492 ± 0.015
potassium	0.038 ± 0.011	0.036 ± 0.004	0.023 ± 0.004		0.263 ± 0.008
Ca		0.042 ± 0.017			0.327 ± 0.026

Table 6. Measured yields of various x-ray lines in the potassium spectra of which fig. 5 is an example. $K_s\varepsilon$ is the product of the number of stopped kaons and the detector efficiency. "Blank" represents no Er absorber.

Detector	Absorber (g/cm^2)	$K_s\varepsilon$ (10^6)	K_α + $K^-n=10\to7$	$K_{\beta_1'}+K_{\beta_2'}$ + $K^-n=6\to5$ + $K^-n=8\to6$	$K^-n=10\to7$	K_α	$K_{\beta'}$	$K^-n=6\to5$ + $K^-n=8\to6$	$K^-n=8\to6$	$K^-n=6\to5$	$\frac{K^-n=6\to5}{K_s\varepsilon}$ (10^{-6})
C	"Blank"	1.89	153.2	568	51.4	101.8	25.4	542.6	49.4	493.2	261.1
		±0.05	±25.5	±33	±8.7	±26.9	±6.7	±33.7	±11.3	±35.5	±20.0
	0.123	1.58	440.8	370	24.9	415.9	87.1	282.9	29.0	253.9	161.1
		±0.06	±29.4	±28.5	±4.4	±29.7	±13.0	±34.3	±6.7	±34.9	±23.0
	0.1238	1.94	533.4	442.4	30.4	503	95.1	347.3	35.6	311.7	161.1
		±0.06	±31.4	±29.7	±5.3	±31.8	±19.1	±35.3	±8.2	±36.2	±19.3
	0.237	1.17	305	178.0	11.2	294.2	69.5	108.5	15.5	93	79.6
		±0.06	±23.2	±19.5	±3.7	±23.5	±13.6	±23.8	±3.7	±24	±20.9
D	"Blank"	2.00	104	589.8	53.8	50.2	29.3	560.5	51.0	509.5	255.0
		±0.06	±24.7	±32.3	±9.2	±26.4	±12.0	±34.5	±11.6	±36.4	±19.9
	0.1238	1.62	394.9	338.8	25.2	369.7	112.6	226.2	29.1	197.1	121.7
		±0.06	±28.7	±29.0	±4.5	±29.1	±20.0	±35.2	±6.9	±35.9	±22.6

Table 6. Continued

Detector	Absorber (g/cm^2)	$K_s\varepsilon$ (10^6)	K_α + $K^-n=10\to7$	$K_{\beta_1'}+K_{\beta_2'}$ + $K^-n=6\to5$ + $K^-n=8\to6$	$K^-n=10\to7$	K_α	$K_{\beta'}$	$K^-n=6\to5$ + $K^-n=8\to6$	$K^-n=8\to6$	$K^-n=6\to5$	$\frac{K^-n=6\to5}{K_s\varepsilon}$ (10^{-6})
D	0.123	2.03 ±0.08	427.6 ±30.9	314.0 ±31.4	31.7 ±5.6	405.1 ±31.3	101.3 ±7.8	212.7 ±32.4	36.3 ±8.4	176.4 ±33.5	86.9 ±16.9
	0.237	2.00 ±0.05	416.1 ±28.4	248.4 ±27.8	18.8 ±3.2	397.3 ±28.6	128.7 ±19.5	119.7 ±34.0	26.0 ±6.0	93.7 ±34.5	46.9 ±17.3
E	"Blank"	1.75 ±0.06	139.2 ±25.7	528.2 ±31.8	47.8 ±8.1	91.4 ±26.9	22.9 ±6.7	505.3 ±32.5	46.0 ±10.5	459.3 ±34.2	262.2 ±21.4
	0.1238	2.08 ±0.08	570.8 ±33.4	462.8 ±30.0	32.8 ±5.7	538.0 ±33.9	134.5 ±8.5	328.3 ±31.2	38.4 ±9.0	289.9 ±32.5	139.6 ±16.5
	0.123	2.07 ±0.05	552.4 ±31.0	427.6 ±29.8	32.8 ±5.6	519.6 ±31.5	129.9 ±7.9	297.7 ±30.8	38.2 ±8.9	259.5 ±32.1	125.6 ±15.8
	0.237	2.33 ±0.05	606.6 ±31.3	397.4 ±27.5	22.3 ±3.7	584.3 ±31.5	146.1 ±7.9	251.3 ±28.6	30.9 ±7.2	220.4 ±29.5	94.7 ±12.8
F	"Blank"	1.14 ±0.06	95.6 ±18	269 ±23	24 ±4.3	71.6 ±18.5	2.9 ±0.74	266.1 ±23.0	24.2 ±5.7	241.9 ±23.7	212.9 ±23.8

Table 6. Continued

Detector	Absorber (g/cm^2)	$K_s\varepsilon$ (10^6)	K_α + $K^-n=10\to7$	$K_{\beta_1'}+K_{\beta_2'}$ + $K^-n=6\to5$ + $K^-n=8\to6$	$K^-n=10\to7$	K_α	$K_{\beta'}$	$K^-n=6\to5$ + $K^-n=8\to6$	$K^-n=8\to6$	$K^-n=6\to5$	$\frac{K^-n=6\to5}{K_s\varepsilon}$ (10^{-6})
	0.1238	2.09	476	443.8	24.1	451.9	165.8	278	29.5	248.5	118.8
		±0.05	±30	±29	±4.4	±30	±21.0	±35.8	±7.1	±36.5	±17.6
	0.123	2.06	461.3	414.2	28.7	432.6	148.1	266.1	29.1	237	114.8
		±0.06	±29.3	±31	±5.2	±29.8	±21.1	±33.7	±7.1	±34.4	±17.0
	0.237	1.72	368.6	218.8	12.0	356.6	102.2	116.6	17.6	99	57.5
		±0.06	±27	±25	±2.3	±27.1	±17.0	±30	±4.2	±30	±17.5

of stopped kaons and detector efficiencies before making any comparisons.

C. Analysis of the Spectrum With an Absorber

The spectrum in fig. 5 corresponding to the detector covered by an absorber was analyzed in the following way. Since the absorbing cross section was five times greater above than below the Er K edge, a drop in the background occurred at the edge. The background below the edge was determined by extrapolating to the edge starting with the background averaged over a 1 keV range 3σ below the centroid of the K_{α_2} line. The background above the edge was determined also by extrapolation starting from an averaged background a few keV away as shown in the fig. 5. Since our detectors could not resolve the edge which had a natural width of about 27 eV, the two above backgrounds were joined together at the edge with a drop that was 1 keV wide, the resolution of our detectors.

The counts under a peak were determined in the same way as in the spectrum without an absorber. However, the number of K^- $n = 10 \rightarrow 7$ and K^- $n = 8 \rightarrow 6$ had to be determined differently because these were x rays that had passed through an absorber. First, the K^- $n = 10 \rightarrow 7$ per stopped kaon without an absorber was determined by taking the K^- $n = 10 \rightarrow 7$ from the spectrum without an absorber and dividing by the number of stopped kaons and the detector efficiency. The number of K^- $n = 10 \rightarrow 7$ per stopped kaon with an absorber was de-

termined by the relation $I = I_0 e^{-\mu t/\rho}$ where μ/ρ is the absorption coefficient at the energy of the line, t is the effective absorber thickness, and I and I_0 are the counts per stopped kaon with and without an absorber, respectively.

$$N_{K^-n = 10 \to 7} = \left[\frac{N_{K^-n = 10 \to 7}}{N_{\text{stopped kaons}} \times \text{detector efficiency}} \right]_{\text{without absorber}} \times$$

$$e^{-\mu t/\rho_{K^-n=10\to7}} \times \left[N_{\text{stopped kaons}} \times \text{detector efficiency} \right]_{\text{absorber}} \qquad (12)$$

The number of K^- n = 8 → 6 was calculated in a similar way.

$$N_{K^-n = 8 \to 6} = \left[\frac{N_{K^-n = 8 \to 6}}{N_{\text{stopped kaons}} \times \text{detector efficiency}} \right]_{\text{without absorber}} \times$$

$$e^{-\mu t/\rho_{K^-n=8\to6}} \times \left[N_{\text{stopped kaons}} \times \text{detector efficiency} \right]_{\text{absorber}} \qquad (13)$$

The absorption coefficients $\mu/\rho_{K^-n=10\to7}$ and $\mu/\rho_{K^-n=8\to6}$ were 4.35 and 2.82 cm^2/g, respectively. Table 6 lists the yields of K^- n = 10 → 7, $K_{\alpha_1} + K_{\alpha_2}$, $K_{\beta_1'} + K_{\beta_2'}$, K^- n = 8 → 6, and K^- n = 6 → 5 measured for each detector with an absorber.

The same procedures that were used to analyze the natural potassium spectra with and without an absorber as described in this chapter were applied to the potassium-41 spectra. The number of K^- n = 10 → 7, $K_{\alpha_1} + K_{\alpha_2}$, $K_{\beta_1'} + K_{\beta_2'}$, K^- n = 8 → 6, and K^- n = 6 → 5 are tabulated in table 17.

The above numbers should be normalized by the corresponding amount of stopped kaons and detector efficiency before comparing with other spectra.

V. RESULTS OF CASCADE CALCULATION

A. Description of a Mesonic Cascade Program

In the history of mesons cascading in an atom at large n values, mesonic Auger or nonradiative transitions of $n_{initial} - n_{final} = 1$ are dominant. In Godfrey's program the nonradiative rates were determined according to R.A. Ferrell[26] by the nuclear internal conversion coefficients. This model was valid when mesonic orbits were close to the nucleus. To remove this restriction the programs of Seki and of the Columbia group used the formulae of several authors,[27,28,29] who applied perturbation theory to calculate the nonradiative rate. The rate was calculated by using Fermi's Golden Rule No. 2 (transitional probability rate) with the coulomb repulsion as the interaction hamiltonian between the charge of a single electron and the meson. The total nonrelativistic initial wavefunction applied to the Rule represented an electron in its ground state with the meson in an $(n,\ell)_{initial}$ state. The total nonrelativistic final wavefunction represented the meson in a lower $(n,\ell)_{final}$ state with an electron in the continuum.

For the mesonic electric dipole radiative transitions the three programs used the radiative rate formula of Bethe and Salpeter.[30] The rate was proportional to the transitional energy cubed which implied that for radiative transitions the meson would

favor large $n_{initial} - n_{final}$ values.

The Klein-Gordon equation expresses the energies of states with principal quantum numbers n and orbital angular momenta ℓ. Transitions occur between states where ℓ changes by ± 1. In the case of K^- $n = 6 \rightarrow 5$ the transitions were made up of several components of slightly different energies that were unresolved by our detectors. The component of highest intensity occurred between states with maximum orbital momenta (circular, $\ell_{initial} = 5$ to $\ell_{final} = 4$). Other components which had lower intensities were contributed by transitions among states of orbital momenta less than the maximum (noncircular). The lines from noncircular transitions were considered as interfering lines because their mass absorption values did not lie on the Er K edge; hence the x-ray intensities had to be corrected.

In order to determine the number of counts contributed by noncircular transitions, a reliable mesonic cascade computer program was needed. Such a program should contain radiative, nonradiative and nuclear strong interaction rates which govern the way kaons cascade through the atom. If the program were written properly, predictions of x-ray intensities would agree with measured mesonic x-ray intensities. The cascade programs considered were written by Dr. Gary L. Godfrey,[25] Prof. Ryoichi Seki and one kindly given by Prof. C.S. Wu's group at Columbia University.

B. Results

Eisenberg and Kessler[27] published a paper with calculations of the intensity ratios

$$\frac{n = 2 \to 1}{n = 2 \to 1 + \sum_{n'>2} n = n' - 1} \quad \text{and} \quad \frac{n = 3 \to 1}{n = 3 \to 1 + \sum_{n'>3} n = n' - 1} \tag{14}$$

which agreed with muonic data of several light elements including potassium. It was tempting to apply the Eisenberg and Kessler calculations to kaons with certain modifications. For transitions between two different n states we considered combining the components contributed by the muon spin. Furthermore muons are not affected by nuclear strong interaction, whereas kaons are affected. By turning off the strong interaction and replacing the kaonic mass by the muonic mass in the programs devised for kaons we could compare the calculations among Eisenberg and Kessler, Godfrey, Seki and Columbia. From these comparisons one learned whether other atomic processes were included besides the radiative and nonradiative processes. Table 7 shows the population of muons in the various orbital angular momentum states for n = 6 from the four programs. For example, by removing the electron refilling process from the Columbia program, the Columbia program then agreed with Eisenberg and Kessler, Godfrey and Seki.

We used Seki's and Godfrey's cascade programs to compare their x-ray intensity ratios of several kaonic atoms with those calculated and measured by G. Backenstoss et al.[31] In the case of kaonic Ca

Table 7. Population of muons that landed into the various orbital angular momentum states of n = 6 in silicon.

Orbital angular momentum ℓ =	0	1	2	3	4	5
Eisenberg and Kessler[27]	74	199	230	279	360	538
Seki	59	187	229	280	363	550
Godfrey	48	156	199	256	360	684
Columbia (e^- refilling included)	15	80	139	229	351	561
Columbia (e^- refilling removed)	63	183	235	288	374	571

Seki's and Godfrey's intensity ratios agreed with the cascade results of G. Backenstoss et al.[31] if the following changes were made in Seki's and Godfrey's programs. The nuclear strong interaction process was turned off and an initial kaonic distribution of $(2\ell+1)\ e^{(\alpha + 0.1)\ell}$ was used instead of $(2\ell+1)\ e^{\alpha\ell}$. The parameter α was assumed to take into account the electron refilling process or any other applicable processes not contained in the cascade program. An initial kaonic distribution was given to the orbital angular momentum ℓ states starting at n = 30. Table 8 displays the intensity ratios of the three programs for α = 0.0 and -0.1. The measured relative intensities listed in the table agreed with the calculated ratios for α = 0.0.

The intensity ratios of kaonic Ca had been normalized to the $n = 6 \rightarrow 5$ in table 8. In order to obtain absolute intensities (x rays per stopped kaon) to compare with Godfrey's measured results, the intensity ratios of G. Backenstoss et al.[31] were multiplied by the absolute intensity of the $n = 6 \rightarrow 5$ which was 0.474 for α = 0.0 in Backenstoss et al.'s cascade calculations. Backenstoss', Godfrey's and Seki's cascade calculations were then compared with the measured values of Godfrey[25] as shown in table 9. With nuclear strong interaction removed Backenstoss', Godfrey's and Seki's cascade results were two times greater than Godfrey's measured values. Putting the nuclear strong interaction back into Godfrey's and Seki's cascade calculations and using an effective kaon-nucleon absorptive scattering length of 0.83 fermi,[25] the two cascade programs still could not fit Godfrey's data as revealed in table 9. The calculated intensities

Table 8. Calculated and measured intensity ratio of $K^{-}Ca$ x rays. Column 2 lists the measured ratios and column 3 lists the weighed averages of the ratios from column 2.

Transition	Backenstoss et al.[31] Intensity ratio	weighed av.	$\alpha = 0.0$ $(2\ell+1)e^{\alpha\ell}$ Backenstoss et al.[31]	$\alpha = 0.0$ $(2\ell+1)e^{(\alpha+.1)\ell}$ Godfrey	$\alpha = 0.0$ $(2\ell+1)e^{(\alpha+.1)\ell}$ Seki	$\alpha = -0.1$ $(2\ell+1)e^{\alpha\ell}$ Backenstoss et al.[31]	$\alpha = -0.1$ $(2\ell+1)e^{(\alpha+.1)\ell}$ Godfrey	$\alpha = -0.1$ $(2\ell+1)e^{(\alpha+.1)\ell}$ Seki
9 → 6	11.2 ± 1.7 4.3 ± 0.7	5.3 ± 0.6	5.2	4.5	5.6	9.75	8.2	9.4
5 → 4	117.6 ± 3.7 126.4 ± 4.4	121.2 ± 2.8	120	120	123	130	127	130
8 → 5	3.4 ± 0.6 6.2 ± 0.3	5.6 ± 0.3	6.4	6.0	7.4	11.9	10.3	12.0
9 → 5	2.8 ± 0.6 3.9 ± 1	3.1 ± 0.5	3.5	2.9	3.6	7.8	5.9	7.2
10 → 5	3.3 ± 0.6 1.26 ± 0.85	2.6 ± 0.5	2.16	1.4	2.0	5.6	3.5	4.6
6 → 4	15.2 ± 1 11.65 ± 1.2	13.7 ± 0.8	15.8	16.0	18.5	26.6	23.7	26.6

Table 8. Continued

Transition	Backenstoss et al.[31] Intensity ratio	weighed av.	$\alpha = 0.0$ $(2\ell+1)e^{\alpha\ell}$ Backenstoss et al.[31]	$(2\ell+1)e^{(\alpha+.1)\ell}$ Godfrey	Seki	$\alpha = -0.1$ $(2\ell+1)e^{\alpha\ell}$ Backenstoss et al.[31]	$(2\ell+1)e^{(\alpha+.1)\ell}$ Godfrey	Seki
7 → 4	3.4 ± 1 4.95 ± 1.2	4.0 ± 0.8	5.9	5.2	6.9	11.9	9.6	11.3
6 → 5	100.7	100.7	100	100	100	100	100	100
7 → 6				75.8	74.6		74.2	73.1
7 → 5				17.0	19.0		23.1	25.3

Table 9. Calculated and measured absolute intensities of $K^{-}Ca$ x rays.

Transition	$\alpha \approx 0.0$; no strong interaction			$\alpha = 0.0$; strong interaction		measured
	Backenstoss et al.[31]	Godfrey	Seki	Godfrey	Seki	Godfrey[25]
9 → 6		0.025	0.028	0.0218	0.0233	
5 → 4	0.565	0.665	0.608	0.373	0.336	0.327 ± 0.055
8 → 5		0.033	0.037	0.025	0.026	
9 → 5		0.016	0.018	0.010	0.012	
10 → 5		0.0078	0.0098	0.0046	0.0055	
6 → 4		0.088	0.092	0.034	0.035	
7 → 4		0.029	0.033	0.0090	0.0099	
6 → 5	0.474	0.554	0.496	0.512	0.452	0.324 ± 0.054
7 → 6		0.420	0.370	0.409	0.358	0.193 ± 0.055
7 → 5		0.094	0.095	0.077	0.077	0.042 ± 0.018

were still two times greater than the measured intensities except for th $n = 5 \rightarrow 4$. The calculated intensity ratio $n = 5 \rightarrow 4 \; / \; n = 6 \rightarrow 5$ from Godfrey and Seki was now 0.07 while the measured was still 1.0. Godfrey[25] had tried to used a $(2\ell+1)$ initial kaonic distribution at $n = 30$ with a cutoff at a certain ℓ value in order to have the cascade calculations yield $n = 5 \rightarrow 4 \; / \; n = 6 \rightarrow 5 = 1$. However, Godfrey's $\Delta n = n_{initial} - n_{final} > 1$ intensities became two times greater than the measured values.

We investigated the above problem further by studying S which had been measured extensively by Wiegand and Godfrey.[5] Various initial kaonic distributions beginning at $n = 30$ were tried. For example, using $(2\ell+1)\, e^{\alpha\ell}$ as the initial distribution a value for α could not be found for Seki's, Godfrey's or the Columbia's program which would give x-ray intensities that fitted all the measured data. A value of α between -0.1 and -0.3 would fit the $n_{initial} - n_{final} > 1$ transitions and a value of α between 0.1 and 0.5 would fit the $n_{initial} - n_{final} = 1$ transitions. But neither values of α would fit the $n = 4 \rightarrow 3$ S line broadened by nuclear absorption. An initial kaonic distribution given in table 10 consisting of a combination of $\alpha = -0.1$ and 0.5 was attempted. Except for the $n = 4 \rightarrow 3$ good agreement with the data was achieved when an effective kaon-nucleon absorptive scattering length of 0.83 fermi[31] was used. However if the scattering length were reduced to approximately 0.2 fermi, all S intensities including the $n = 4 \rightarrow 3$ would agree with the data. Table 10 shows the results and the x-ray intensities of the circular and noncircular $n = 6 \rightarrow 5$ transitions.

Table 10a. Starting initial kaonic distribution for S for the various ℓ orbital angular momentum states of n = 30 in Seki's, Godfrey's and Columbia's cascade programs.

ℓ :	0	1	2	3	4	5	6	7	8	9	10	11	12	13	14	15	16	17	18	19	20	21	22	23	24
K^- population :	1	3	4	5	6	6	7	7	8	8	8	8	8	7	7	7	7	6	6	6	5	5	5	4	4

ℓ :	25	26	27	28	29
K^- population :	4	4	20	30	59

Table 10b. Calculated absolute x-ray intensities of S from Seki's cascade program. Godfrey's and Columbia's cascade programs produced similar results to Seki's. The measured absolute x-ray intensities (x-rays per stopped kaon) were taken from Godfrey's work.[25]

Transition	Calculated	Measured
n=7→6	0.228	0.237 ± 0.042
n=8→6 + n=6→5	0.380	0.364 ± 0.055
n=5→4	0.412	0.361 ± 0.054
n=4→3	0.050	0.047 ± 0.008
n=7→5	0.036	0.040 ± 0.006
n=6→4	0.035	0.039 ± 0.006
n=9→6	0.0096	0.008 ± 0.002
n=8→5	0.014	0.013 ± 0.002
n=7→4	0.013	0.015 ± 0.003
n=9→5	0.008	0.006 ± 0.001
n=8→4	0.008	0.006 ± 0.002

Table 10c. Calculated absolute x-ray intensities (x rays per stopped kaon) of S for the circular and noncircular transitions of $n = 6 \rightarrow 5$ from Seki's cascade program.

Transition :	$6s \rightarrow 5p$	$6p \rightarrow 5s$ + $6p \rightarrow 5d$	$6d \rightarrow 5p$ + $6d \rightarrow 5f$	$6f \rightarrow 5d$ + $6f \rightarrow 5g$	$6g \rightarrow 5f$	$6h \rightarrow 5g$
	2.23×10^{-13}	2.23×10^{-13}	2.59×10^{-8}	0.0003	0.0278	0.3276

Other various kaonic distributions were tried at n = 30 with an absorptive scattering length of 0.83 fermi. None of the attempts gave reasonable x-ray intensities which agreed with the data.

Since we found a set of initial conditions, i.e., an initial kaonic distribution and an effective kaon-nucleon scattering length which allowed Seki's and Godfrey's cascade programs to predict x-ray intensities close to the measured values of S, we tried Seki's cascade program on potassium with the same set of initializations. The only changes in the cascade programs were to use the K and L electronic binding energies of Ar instead of P in the calculations of the nonradiative rates of potassium and to use atomic number 19 instead of 16. The calculated potassium intensities are shown in table 11. The table includes a breakdown of the circular and noncircular x-ray intensities of K^- $n = 6 \rightarrow 5$. Since there was a possibility that the agreement with the measured data could be improved, we altered the initial kaonic distribution and the effective kaon-nucleon scattering length in search for better results. Table 11 and 12 shows the initial kaonic distributions tried with their calculated intensities. Distributions C and H appeared to have the closest match. However, none of the initializations yielded x-ray intensities in close agreement with the measured data as in the S case. From table 12 for those sets of initializations which came close to agreeing with the measured potassium data, the calculated ratio of noncircular to total K^- $n = 6 \rightarrow 5$ was in the neighborhood of 10%. Similarly an 8% ratio was found for S as revealed in table 10.

Table 11a. Calculated absolute x-ray intensities of potassium from Seki's cascade program. The measured absolute x-ray intensities (x rays per stopped kaon) were taken from Godfrey's work.[25]

Transition	Measured	A	B	C	D	E	F	G	H
n=7→6	0.146 ± 0.027	0.309	0.319	0.263	0.266	0.195	0.202	0.185	0.155
n=8→6 + n=6→5	0.285 ± 0.044	0.447	0.450	0.384	0.388	0.307	0.316	0.291	0.221
n=5→4	0.263 ± 0.040	0.434	0.332	0.283	0.287	0.226	0.232	0.214	0.180
n=9→7	0.038 ± 0.012	0.021	0.019	0.024	0.025	0.035	0.035	0.033	0.026
n=7→5	0.036 ± 0.006	0.040	0.035	0.043	0.042	0.059	0.060	0.057	0.043
n=6→4	0.023 ± 0.005	0.034	0.020	0.025	0.025	0.034	0.034	0.032	0.026
n=10→7	0.023 ± 0.007	0.009	0.008	0.010	0.011	0.014	0.013	0.013	0.012
n=9→6	0.015 ± 0.004	0.014	0.012	0.016	0.017	0.023	0.023	0.021	0.018
n=8→5	0.013 ± 0.004	0.016	0.013	0.018	0.020	0.027	0.027	0.025	0.020
Effective kaon-nucleon scattering length tried (fermi) :		0.15	0.83	0.83	0.83	0.83	0.83	0.83	0.83

Table 11b. Calculated absolute x-ray intensities (x rays per stopped kaon) of potassium for the circular and noncircular transitions of n = 6 → 5 from Seki's cascade program.

Transition :	6s → 5p	6p → 5s + 6p → 5d	6d → 5p + 6d → 5f	6f → 5d + 6f → 5g	6g → 5f	6h → 5g
A	3.14×10^{-14}	3.14×10^{-14}	3.68×10^{-9}	8.48×10^{-5}	0.0271	0.3866
B	5.68×10^{-16}	5.68×10^{-16}	9.65×10^{-11}	9.15×10^{-6}	0.0161	0.4042
C	6.12×10^{-16}	6.12×10^{-16}	1.05×10^{-10}	1.12×10^{-5}	0.0202	0.3256
D	5.95×10^{-16}	5.95×10^{-16}	1.03×10^{-10}	1.15×10^{-5}	0.0203	0.3292
E	6.19×10^{-16}	6.19×10^{-16}	1.10×10^{-10}	1.43×10^{-5}	0.0279	0.2242
F	6.75×10^{-16}	6.75×10^{-16}	1.09×10^{-10}	1.37×10^{-5}	0.0277	0.2336
G	7.56×10^{-16}	7.56×10^{-16}	1.18×10^{-10}	1.36×10^{-5}	0.0265	0.2132
H	8.22×10^{-16}	8.22×10^{-16}	1.40×10^{-10}	1.38×10^{-5}	0.0210	0.1821

Table 12. Starting initial kaonic distribution for potassium for the various ℓ orbital angular momentum states of n = 30 in Seki's cascade programs.

Distribution A	ℓ :	0	1	2	3	4	5	6	7	8	9	10	11	12	13	14	15	16	17	18	19	20	21	22
K^- population :		1	3	4	5	6	6	7	7	8	8	8	8	8	7	7	7	7	6	6	6	5	5	5
	ℓ :	23	24	25	26	27	28	29																
K^- population :		4	4	4	4	20	30	59																
Distribution B	ℓ :	0	1	2	3	4	5	6	7	8	9	10	11	12	13	14	15	16	17	18	19	20	21	22
K^- population :		1	3	4	5	6	6	7	7	8	8	8	8	8	7	7	7	7	6	6	6	5	5	5
	ℓ :	23	24	25	26	27	28	29																
K^- population :		4	4	4	4	20	30	59																
Distribution C	ℓ :	0	1	2	3	4	5	6	7	8	9	10	11	12	13	14	15	16	17	18	19	20	21	22
K^- population :		1	3	4	5	6	6	7	7	8	8	8	8	8	7	7	7	7	6	6	6	5	5	15
	ℓ :	23	24	25	26	27	28	29																
K^- population :		14	4	4	4	10	20	40																
Distribution D	ℓ :	0	1	2	3	4	5	6	7	8	9	10	11	12	13	14	15	16	17	18	19	20	21	22
K^- population :		1	3	4	5	6	6	7	7	8	8	8	8	8	7	7	7	7	6	6	6	5	5	15
	ℓ :	23	24	25	26	27	28	29																
K^- population :		24	4	4	4	3	4	60																

Table 12. Continued

Distribution E	ℓ :	0	1	2	3	4	5	6	7	8	9	10	11	12	13	14	15	16	17	18	19	20	21
K^- population :		1	3	4	5	6	6	7	7	8	8	8	8	8	7	7	7	7	6	6	6	5	5
	ℓ :	22	23	24	25	26	27	28	29														
K^- population :		45	24	4	4	4	3	4	20														
Distribution F	ℓ :	0	1	2	3	4	5	6	7	8	9	10	11	12	13	14	15	16	17	18	19	20	21
K^- population :		1	3	4	5	6	6	7	7	7	7	7	7	7	6	6	6	5	4	3	3	5	5
	ℓ :	22	23	24	25	26	27	28	29														
K^- population :		45	24	3	3	3	3	4	20														
Distribution G	ℓ :	0	1	2	3	4	5	6	7	8	9	10	11	12	13	14	15	16	17	18	19	20	21
K^- population :		1	3	4	5	5	5	7	7	7	7	7	7	7	6	6	6	5	4	3	3	5	5
	ℓ :	22	23	24	25	26	27	28	29														
K^- population :		25	24	4	4	4	3	4	13														
Distribution H	ℓ :	0	1	2	3	4	5	6	7	8	9	10	11	12	13	14	15	16	17	18	19	20	21
K^- population :		1	3	4	5	6	6	7	7	8	8	8	8	8	7	7	7	7	6	6	6	5	5
	ℓ :	22	23	24	25	26	27	28	29														
K^- population :		9	7	4	4	4	3	4	13														

Energies of the $K^-n = 6 \rightarrow 5$ noncircular transitions contained only the Klein-Gordon and the first order ($\alpha Z\alpha$) vacuum polarization terms. According to table 13 which lists the calculated energies of the K^- $n = 6 \rightarrow 5$ noncircular transitions, the $6g \rightarrow 5f$ (57525 eV) and the $6f \rightarrow 5d$ (57600 eV) transitions had energies above the Er K edge (57486 eV). Observing tables 11 and 12 we note that for those initial conditions which agreed with the measured data, practically all noncircular x-ray intensities came from the $6g \rightarrow 5f$ and the $6f \rightarrow 5d$. We neglected, in correcting our measured μ/ρ for noncirculars, the $6d \rightarrow 5p$, $6p \rightarrow 5s$ and all $\Delta\ell = \ell_{initial} - \ell_{final} = -1$ transitions which altogether contributed less than 1% of the noncircular intensities.

The profile of the Er K edge had been measured by Fairchild.[34] The data at the edge was fitted with an arctangent curve of the form[32]

$$\mu/\rho(cm^2/g) = \mu/\rho_< + (\mu/\rho_> - \mu/\rho_<) \left[1/2 - \pi^{-1} \tan^{-1} \left\{ \frac{2(E_0-E)}{\Gamma} \right\} \right] \quad (15)$$

where $\mu/\rho_<$ and $\mu/\rho_>$ are the mass absorption coefficient values below and above the edge. The data gave $\mu/\rho_<$ and $\mu/\rho_>$ to be 2.7 cm^2/g and 10.4 cm^2/g, respectively. McMaster et al.[22] gave $\mu/\rho_<$ and $\mu/\rho_>$ to be 2.81 cm^2/g and 15.00 cm^2/g. Furthermore, we had measured 13.73 $\pm$ 0.03 cm^2/g at 59.5 keV: 3.3 cm^2/g higher than the maximum which Fairchild had measured. Because of this problem we chose $\mu/\rho_<$ and $\mu/\rho_>$ to be 2.81 and 15.00 cm^2/g, respectively as taken from McMaster et al.[22] The μ/ρ values included the photoelectric and incoherent processes. E_0, the Er K electron binding energy is 57486 eV[33] (the inflection point

Table 13. Calculated energies of the K^- $n = 6 \rightarrow 5$ noncircular and circular transitions. The noncircular transitions contained only the Klein-Gordon and the first order ($\alpha Z\alpha$) vacuum polarization terms. The circular $6h \rightarrow 5g$ contains the Klein-Gordon, the vacuum polarization terms ($\alpha(Z\alpha)$, $\alpha^2(Z\alpha)$, $\alpha(Z\alpha)^3$, $\alpha(Z\alpha)^5$, $\alpha(Z\alpha)^7$), nuclear finite size, the shift due to nuclear strong interaction, and the electron screening correction. Table 15 lists the constants used in the above calculations.

$\Delta\ell = \ell_{initial} - \ell_{final} = 1$:				
$6p \rightarrow 5s$	$6d \rightarrow 5p$	$6f \rightarrow 5d$	$6g \rightarrow 5f$	$6h \rightarrow 5g$
38115 eV	56244 eV	57600 eV	57525 eV	57469 eV
$\Delta\ell = \ell_{initial} - \ell_{final} = -1$:				
$6s \rightarrow 5p$	$6p \rightarrow 5d$	$6d \rightarrow 5f$	$6f \rightarrow 5g$	
67839 eV	58261 eV	57379 eV	57354 eV	

of the arctangent curve, equation 15). Although there is some uncertainty as to how wide the absorption width Γ of the edge is we have taken Γ to be 27.5 eV as measured by Fairchild.[34] Inserting the values of $\mu/\rho_<$(2.81 cm^2/g), $\mu/\rho_>$(15.00 cm^2/g), E_0(57486 eV) and Γ (27.5 eV) into equation 15, fig. 9 displays the shape of the curve we have adopted for the Er K edge at present.

The appropriate number of counts contributed by 10% noncircular transitions was remove from the $K^-n = 6 \rightarrow 5$ spectra with and without an absorber. From fig. 9 we see that the energies of the $6g \rightarrow 5f$ and $6f \rightarrow 5d$ transitions corresponded to a μ/ρ of 14.3 cm^2/g. For example, from table 6 before any noncircular corrections were made, the x rays per stopped kaons of detector C were 261.1 $\pm$ 20.0, 161.1 $\pm$ 23.0, 161.1 $\pm$ 19.3, 79.6 $\pm$ 20.9 for no absorber, 0.126 cm^2/g, 0.126 cm^2/g and 0.243 cm^2/g absorbers, respectively (effective thicknesses have been used). Corresponding to the above values, μ/ρ was 4.25 $\pm$ 0.61 cm^2/g. Assuming that now 10% of the $K^-n = 6 \rightarrow 5$ were noncirculars, the x rays per stopped kaons would be 235.0 $\pm$ 20.1, 156.7 $\pm$ 23.0, 156.7 $\pm$ 19.3 and 78.8 $\pm$ 20.9 and μ/ρ would become 3.76 $\pm$ 0.61 cm^2/g. Table 14 shows after averaging over our results from the four detectors that our measured μ/ρ was 4.74 $\pm$ 0.29 cm^2/g before and 4.27 $\pm$ 0.29 cm^2/g after correcting for a 10% contribution of noncirculars.

Prior to performing our experiment we had calculated where the energy of the $6h \rightarrow 5g$ transition would lie on the Er K edge. We had used a kaonic mass m_K of 493.707 MeV as published in the Review of Particle Properties' tables.[35] The mass was inserted into the reduced mass

Fig. 9 Calculated Er K edge using equation 15 with $\mu/\rho_{<}$(2.81 cm^2/g), $\mu/\rho_{>}$(15.00 cm^2/g), E_0(57486 eV) and Γ(27.5 eV).

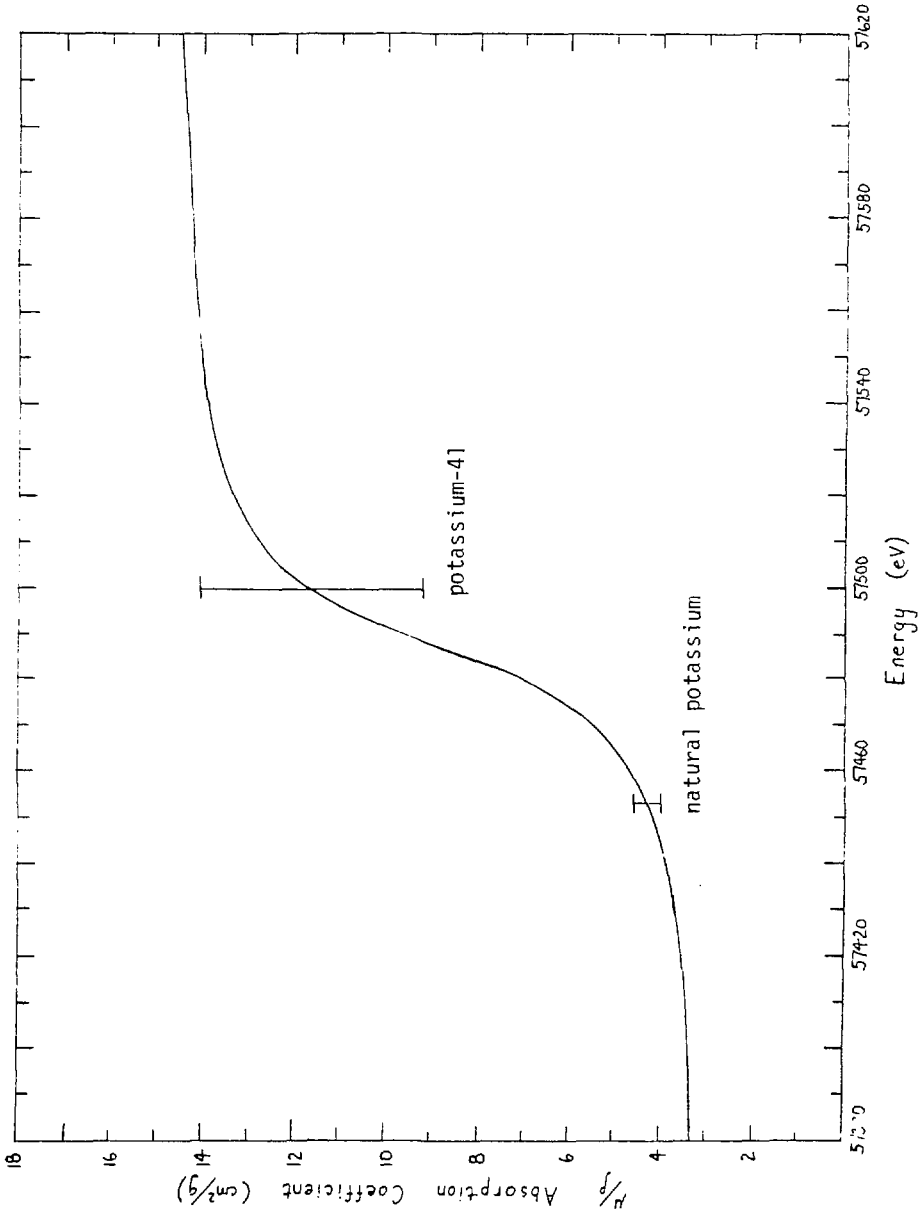

Table 14. Measured values of $\mu/\rho(cm^2/g)$. Column 2 lists the μ/ρ values of each detector before correcting for noncircular transitions. Columns 3, 4, 5 list the μ/ρ values corrected for 10%, 15% and 20% noncircular transitions. The energies corresponding to the weighed averages of the measured μ/ρ values were taken from fig. 9. The kaon mass was determined by inserting the energy $E_{meas.}$ into equation 16.

% of noncirculars	0%	10%	15%	20%
Detector	(cm^2/g)	(cm^2/g)	(cm^2/g)	(cm^2/g)
C	4.25 ± 0.61	3.76 ± 0.61	3.48 ± 0.63	3.21 ± 0.61
D	7.02 ± 0.88	6.55 ± 0.88	6.29 ± 0.89	6.02 ± 0.89
E	4.36 ± 0.42	3.89 ± 0.42	3.64 ± 0.43	3.46 ± 0.42
F	5.00 ± 0.69	4.53 ± 0.69	4.26 ± 0.71	4.01 ± 0.71
Weighed average :	4.74 ± 0.29	4.27 ± 0.29	4.01 ± 0.30	3.77 ± 0.29
$E_{meas.}$ (eV)	57462^{+4}_{-4}	57454^{+5}_{-8}	57446^{+9}_{-11}	57438^{+10}_{-18}
m_K (MeV)	$493.646^{+0.035}_{-0.035}$	$493.576^{+0.044}_{-0.069}$	$493.507^{+0.078}_{-0.096}$	$493.437^{+0.087}_{-0.157}$

Table 15. Constants used in the energy calculation of the $K^-n = 6 \rightarrow 5$ circular and noncircular transitions.

Kaon mass $m_{K^-} = 493.707$ MeV

Fine structure $\alpha = 1/137.035982$

Electron mass $m_e = 511.0034$ keV

Atomic mass of natural potassium $M_{{}^{39}_{19}K} = 39.09$ amu

Atomic mass of isotopic potassium-41 $M_{{}^{41}_{19}K} = 40.9618$ amu

1 amu = 931.5016 MeV

$m_K m_A/(m_K + m_A)$ contained in each of the following terms: the Klein Gordon expression, the vacuum polarization terms ($\alpha(Z\alpha)$, $\alpha^2(Z\alpha)$, $\alpha(Z\alpha)^3$, $\alpha(Z\alpha)^5$, $\alpha(Z\alpha)^7$), nuclear finite size, the shift due to nuclear strong interaction, and the electron screening correction. The calculated energy of the $K^-n = 6h \rightarrow 5g$ in natural potassium was 57469 eV. The calculated energies of the above terms are listed in table 16.

In order to determine the kaon mass based on our measurements of the energy from μ/ρ, we assumed that each of the energy correction terms mentioned above was proportional to the reduced mass, i.e. $E = m_K m_A c^2 B/(m_K + m_A)$, where B is independent of the mass and contains the Klein-Gordon, vacuum polarization terms, nuclear finite size, the shift due to nuclear strong interaction and the electron screening correction. Our measured kaon mass m_K was then related to the energy $E_{meas.}$ by

$$m_K = \frac{m_A}{\left\{\frac{57469\ \text{eV}}{E_{meas.}} \frac{(493.707\ \text{MeV} + m_A)}{493.707\ \text{MeV}} - 1\right\}} \qquad (16)$$

where m_A is the atomic mass (see table 15) and $E_{meas.}$ is the energy corresponding to our measured μ/ρ.

From the μ/ρ versus energy E curve shown in fig. 9 value of $4.74 \pm 0.29\ cm^2/g$ and $4.27 \pm 0.29\ cm^2/g$ corresponded to energies 5746_{-4}^{+4} eV and $57454\ ^{+5}_{-8}$ eV, respectively. Inserting these energies into equation 16 a kaonic mass of $493.646\ ^{+0.035}_{-0.035}$ MeV and $493.576\ ^{+0.044}_{-0.069}$ MeV was determined corresponding to no correction and a correction for 10% non-circulars, respectively.

Table 16. Calculated energy corrections to the Klein-Gordon for potassium-39 and -41. Constants used in the above calculations are listed in table 15.

Element	Transition	Klein-Gordon (eV)	Vacuum Polarization terms $\alpha(Z\alpha)$ (eV)	$\alpha^2(Z\alpha)$ (eV)	$\alpha(Z\alpha)^3$ (eV)	$\alpha(Z\alpha)^5 + \alpha(Z\alpha)^7$ (eV)	Nuclear finite size + strong interaction shift (eV)	Electron screening (eV)	Total (eV)
$^{39}_{19}K$	n=6h → 5g	57252.4	214.4	1.6	-0.34	-0.0023	1	-0.5	57468.6
$^{41}_{19}K$	n=6h → 5g	57287.4	214.6	1.6	-0.34	-0.0023	1	-0.5	57503.8

Since we could not find a set of calculated potassium x-ray intensities which agreed with the measured data of Godfrey,[25] we pursued the analysis further by assuming the possibilities that within the total $K^-n = 6 \rightarrow 5$ intensity either 15% or 20% were noncircular x rays. As listed in table 14 the weighed average μ/ρ from our four detectors for a correction of 15% and 20% noncirculars were 4.01 ± 0.30 cm^2/g and 3.77 ± 0.29 cm^2/g, respectively. From fig. 9 μ/ρ of 4.01 ± 0.30 cm^2/g and 3.77 ± 0.29 cm^2/g corresponded to energies $57446 \begin{smallmatrix}+9\\-11\end{smallmatrix}$ eV and $57438 \begin{smallmatrix}+10\\-18\end{smallmatrix}$ eV and to kaonic masses, $493.507 \begin{smallmatrix}+0.078\\-0.096\end{smallmatrix}$ MeV and $493.437 \begin{smallmatrix}+0.087\\-0.157\end{smallmatrix}$ MeV, respectively. According to table 14 the removal of more noncircular x rays from the $n = 6 \rightarrow 5$ line led to the lowering of the kaon mass.

From our analysis of the potassium-41 spectra as tabulated in table 17 we measured an averaged μ/ρ of 11.9 ± 2.3 cm^2/g for the $K^-n = 6 \rightarrow 5$ line. To correct for noncirculars we assumed 10% of the total $K^-n = 6 \rightarrow 5$ to be noncirculars according to the above calculated cascade results. μ/ρ was then 11.6 ± 2.4 cm^2/g. The energies $E_{meas.}$ corresponding to the above μ/ρ values are displayed in table 18. Inserting $E_{meas.}$ into equation 16 and changing the calculated energy of $6h \rightarrow 5g$ from 57469 eV (natural potassium) to 57504 eV (potassium-41), the kaon mass was $493.674 \begin{smallmatrix}+0.574\\-0.096\end{smallmatrix}$ MeV for no correction of noncirculars and $493.674 \begin{smallmatrix}+0.574\\-0.096\end{smallmatrix}$ MeV for a correction of 10% noncircular x rays.

Table 17. Measured yields of x-ray lines from the isotopic potassium-41 spectra. For potassium-41 the target for the kaon beam consisted of potassium fluoride. $K_{S}\varepsilon$ is the product of the number of stopped kaons and of the detector efficiency. "Blank" represents no Er absorber.

Detector	Absorber (g/cm^2)	$K_{S}\varepsilon$ (10^6)	K_α + $K^-n=10\to7$	$K_{\beta_1'}+K_{\beta_2'}$ + $K^-n=6\to5$ + $K^-n=8\to6$	$K^-n=10\to7$	K_α	$K_{\beta'}$	$K^-n=6\to5$ + $K^-n=8\to6$	$K^-n=8\to6$	$K^-n=6\to5$	$\frac{K^-n=6\to5}{K_{S}\varepsilon}$ (10^{-6})
C	"Blank"	2.61 ±0.02	62 ±23.8	397.8 ±35.7	36.0 ±6.6	26.0 ±24.7	6.5 ±6.2	391.3 ±36.2	35.6 ±6.6	355.7 ±36.8	136.1 ±14.1
	0.123	2.59 ±0.02	552.2 ±43.7	234.2 ±34.4	20.7 ±3.7	531.5 ±43.9	132.9 ±11.0	101.3 ±36.1	24.7 ±4.6	76.6 ±36.4	29.6 ±14.1
D	"Blank"	2.81 ±0.02	106 ±27.0	305.8 ±34.2	27.4 ±5.4	78.6 ±27.5	44.2 ±19.2	261.6 ±39.2	23.8 ±6.3	237.8 ±39.7	84.6 ±14.1
	0.1238	2.86 ±0.02	581.8 ±49.5	241.8 ±30.8	16.0 ±3.1	565.8 ±49.6	184.2 ±23.0	57.6 ±38.4	17.1 ±4.3	40.5 ±38.6	14.2 ±13.5
E	"Blank"	3.00 ±0.02	129.3 ±26.4	370.4 ±34.3	33.5 ±6.2	95.8 ±27.1	0	370.4 ±34.3	33.7 ±8.0	336.7 ±35.2	112.4 ±11.8

Table 17. Continued

Detector	Absorber (g/cm^2)	$K_S\varepsilon$ (10^6)	K_α + $K^-n=10\to7$	$K_{\beta_1'}+K_{\beta_2'}$ + $K^-n=6\to5$ + $K^-n=8\to6$	$K^-n=10\to7$	K_α	$K_{\beta'}$	$K^-n=6\to5$ + $K^-n=8\to6$	$K^-n=8\to6$	$K^-n=6\to5$	$\frac{K^-n=6\to5}{K_S\varepsilon}$ (10^{-6})
E	0.123	3.09 ±0.02	721.2 ±49.2	349.0 ±32.5	20.0 ±3.7	701.2 ±49.4	258.9 ±25.6	90.1 ±41.4	24.4 ±5.9	65.7 ±41.8	21.3 ±13.5
F	"Blank"	2.87 ±0.02	58.8 ±22.5	327.8 ±33.2	29.6 ±5.6	29.2 ±23.2	7.3 ±5.8	298.6 ±40.5	27.2 ±7.0	271.4 ±41.1	94.6 ±14.3
	0.1238	2.94 ±0.02	618.4 ±43.2	271.4 ±29.0	17.6 ±3.5	600.8 ±43.3	177.3 ±21.6	94.1 ±36.2	19.7 ±5.0	74.4 ±36.5	25.3 ±12.4

Table 18. Measured values of $\mu/\rho(cm^2/g)$ of the $K^-n=6h \rightarrow 5g$ from the potassium-41 spectra. Columns 2, 3 list the μ/ρ values of each detector before and after correcting for 10% noncircular transitions. The energies $E_{meas.}$ corresponding to the weighed averages of the measured μ/ρ values were taken from fig. 9 . The kaon mass was determined by inserting the energy $E_{meas.}$ into equation 16 and by replacing 57469 eV by 57504 eV (the calculated energy of the $K^-n=6h \rightarrow 5g$ in potassium-41).

% of noncirculars	0%	10%
Detector	(cm^2/g)	(cm^2/g)
C	12.1 ± 3.9	11.9 ± 4.1
D	13.9 ± 7.4	13.9 ± 8.2
E	13.1 ± 5.0	12.9 ± 5.5
F	10.3 ± 3.9	9.9 ± 4.1
Weighed average :	11.9 ± 2.3	11.6 ± 2.4
$E_{meas.}$ (eV)	57500^{+66}_{-11}	57498^{+48}_{-10}
m_K (MeV)	$493.674^{+0.574}_{-0.096}$	$493.657^{+0.417}_{-0.087}$

VI. CONCLUSION

At the present time the energy of the kaonic 6h → 5g transition has been determined by using the calculated μ/ρ curve as shown in fig. 9. In the future the actual profile of the edge would have to be measured on a calibrated energy scale in order to remove any doubts as to where the 6h → 5g is really located on the μ/ρ curve.

Because our detectors could not resolve the noncircular transitions, we had to depend on the predictions from a calculated cascade program. According to the cascade results for potassium we found that the number of noncircular x rays was about 10% of all the transitions between n = 6 to n = 5. Based on the above available informations we measured the mass of the kaon to be $493.576 \begin{smallmatrix}+0.044\\-0.069\end{smallmatrix}$ MeV.

REFERENCES

1. Clyde E Wiegand and Dick A. Mack, Phys. Rev. Lett. 18, 685 (1967).

2. G. Backenstoss, A. Bamberger, J. Egger, W.D. Hamilton, H. Koch, U. Lynen, H.G. Ritter, and H. Schmitt, Phys. Lett. B32, 399 (1970).

3. P.D. Barnes, R.A. Eisenstein, W.C. Lam, J. Miller, R.B. Sutton, M. Eckhause, J. Kane, R.E. Welsh, D.A. Jenkins, R.J. Powers, R. Kunselman, R.P. Redwine, R.E. Segel, and J.P. Schiffer, Phys. Rev. Lett. 29, 230 (1970).

4. Clyde E. Wiegand, Phys. Rev. Lett. 22, 1235 (1969).

5. Clyde E. Wiegand and Gary L. Godfrey, Phys. Rev. A9, 2282 (1974).

6. S.C. Cheng et al., Bull. Amer. Phys. Soc. 20, 701 (1975).

7. Ryoichi Seki and Clyde E. Wiegand, Ann. Rev. Nucl. Sci. 25, 241 (1975).

8. E.H.S. Burhop, Ed., High-Energy Physics, Vol. III, (Academic, New York-London, 1969), p. 109.

9. Y.N. Kim, Mesonic Atoms and Nuclear Structure (North-Holland, Amsterdam, 1971).

10. G. Backenstoss et al., Phys. Lett. B43, 431 (1973).

11. S.C. Cheng, Y. Asano, M.Y. Chen, G. Dugan, E. Hu, L. Lidofsky, W. Patton, C.S. Wu, V Hughes, D. Lu, Nucl. Phys. A254, 381 (1975).

12. Min-Yi Chen, Phys. Rev. Lett. 34, 341 (1975).

13. L. Wilets and G.A. Rinker, Jr., Phys. Rev. Lett. 34, 339 (1975).

14. G. Backenstoss et al., Phys. Lett. B38, 181 (1972), Nucl. Phys. B73, 189 (1974); H. Koch, Proc. Int. Conf. High Energy Phys. Nucl. Struct., 5th, 225 (1974); A.R. Kunselman, Phys. Lett. B34, 485 (1971);

P.D. Barnes et al., Nucl. Phys. A231, 477 (1974); J. Miller, "An experimental investigation of strong interaction effects in kaonic and antiprotonic atoms", PhD thesis, Carnegie-Mellon Univ., Pittsburgh, Pa. (1974).

15. C.E.Wiegand and G.L. Godfrey, Lawrence Berkeley Lab. Rep. 3080.
16. S.C. Cheng et al., Bull. Am. Phys. Soc. 19, 599 (1974).
17. J.N. Bradbury, M. Leon, H. Daniel, J.J. Reidy, Phys. Rev. Lett. 34, 303 (1975).
18. G.L. Godfrey, G.K. Lum, C.E. Wiegand, Lawrence Berkeley Lab. Rep. 3616 (1975).
19. F. Iachello, A. Lande, Phys. Lett. B35, 205 (1971); T.E.O. Ericson, J. Hufner, Phys. Lett. B40, 459 (1972); Nucl. Phys. B47, 205 (1972); U.E. Schroder, Acta Phys. Austr. 36, 248 (1972).
20. C.E. Wiegand, G.K. Lum, G.L. Godfrey, Phys. Rev. 15, 1780 (1977).
21. Richard H. Pehl and Fred S. Goulding, Nucl. Instrum. Methods 81, 329 (1970).
22. W.H. McMaster, N. Kerr Del Grande, J.H. Mallet, and J.H. Hubbell, Lawrence Radiation Laboratory Report No. UCRL-50174, 1969 (unpublished).
23. E. Storm and H.I. Israel, Nucl. Data A7, 565 (1970).
24. C.M. Lederer, J.M. Hollander, and I. Perlman, Table of Isotopes (Wiley, New York, 1967).
25. G.L. Godfrey, Lawrence Berkeley Laboratory Rep. LBL-3857, 1975 (unpublished).
26. Richard A. Ferrell, Phys. Rev. Lett. 4, 425 (1960).

27. Y. Eisenberg and D. Kessler, Nuovo Cimento 19, 1195 (1961); Phys. Rev. 123, 1472 (1961); Phys. Rev. 130, 2352 (1963).

28. G.R. Burbidge and A.H. de Borde, Phys. Rev. 89, 189 (1953).

29. A.H. de Borde, Proc. Roy. Soc. London 67, 57 (1954).

30. H.A. Bethe and E.E. Salpeter, Quantum Mechanics of One- and Two-Electron Atoms (Academic, New York, 1957), equation 63.2, p. 348.

31. G. Backenstoss, T. Bunaciu, J. Eggar, H. Koch, A. Schwitter, and L. Tauscher, Z. Physik A273, 137 (1975).

32. F.K. Richtmeyer, S.W. Barnes, and E. Barnes, Phys. Rev. 46, 843 (1934).

33. P. Bergvall and S. Hagström, Arkiv f. Fysik 17, 61 (1959).

34. R.W. Fairchild, PhD thesis, Cornell University, 1975 (unpublished).

35. Review of Particle Properties, Particle Data Group, Rev. Mod. Phys. 48, S1 (1976).